ARIZONA DEPARTMENT OF TRANSPORTATION

REPORT NUMBER: FHWA-AZ87-254

RATIONAL CHARACTERIZATION OF PAVEMENT STRUCTURES USING DEFLECTION ANALYSIS

Volume I - Research Results & Findings

Final Report

Prepared by:
Michael S. Mamlouk
William N. Houston
[redacted]
Sandra L. Houston
John P. Zaniewski

Center for Advanced Research in Transportation, and
Department of Civil Engineering
College of Engineering & Applied Sciences
Arizona State University
Tempe, Arizona 85287

December 1988

Prepared for:
Arizona Department of Transportation
206 South 17th Avenue
Phoenix, Arizona 85007
in cooperation with
U.S. Department of Transportation
Federal Highway Administration

Technical Report Documentation Page

1. Report No.	2. Government Accession No.	3. Recipient's Catatlog No.
FHWA-AZ88-254,I		

4. Title and Subtitle

RATIONAL CHARACTERIZATION OF PAVEMENT STRUCTURES USING DEFLECTION ANALYSIS

5. Report Date
December, 1988

6. Performing Organization Code

7. Author(s) Michael S. Mamlouk, William N. Houston, Sandra L. Houston, John P. Zaniewski

8. Performing Organization Report No.
CART-88-101

9. Performing Organization Name and Address

Center for Advanced Research in Transportation
Arizona State University
Tempe, AZ 85287-6306

10. Work Unit No.

11. Contact or Grant No.
HPR-PL-1(31) Item 254

12. Sponsoring Agency Name and Address

ARIZONA DEPARTMENT OF TRANSPORTATION
206 S. 17TH AVENUE
PHOENIX, ARIZONA 85007

13. Type of Report & Period Covered
Vol I-Final Rept 8/86-12/88

14. Sponsoring Agency Code

15. Supplementary Notes

Prepared in cooperation with the U.S. Department of Transportation, Federal Highway Administration

16. Abstract

In this study, a rational overlay design method for flexible pavements in Arizona has been developed which includes roughness, fatigue and plastic deformation models. The method is incorporated in a microcomputer program which is also capable of analyzing the economics of other rehabilitation alternatives.

During the development of the method, twenty in-service pavement sites were selected from Arizona highways covering various geographical and environmental regions, soil types, pavement conditions and traffic volumes. Nondestructive tests (NDT) were performed on these sites using the Falling Weight Deflectometer at three stress levels as well as the Dynaflect. The pavement layers and subgrade moduli were backcalculated from NDT data using both static and dynamic analyses. The moduli of asphaltic layers were further adjusted for temperature. Statistical analysis was performed and the stress sensitivity was found to be small. Cone penetration tests were further performed to verify the subgrade moduli.

Asphalt concrete cores, base and subbase samples and undisturbed subgrade samples were collected from the selected sites. Resilient modulus tests were performed in the lab on asphalt concrete cores at three temperatures and on subgrade materials. In addition, base and subbase gradation as well as soil classification and Atterberg limits were obtained. The study expanded the data base for material properties in Arizona.

This volume is the first in a three volume set. Volume II provides field testing procedure and workstation development and Volume III is a computer user guide.

23. Registrant's Seal

Registered Professional Engineer (Civil)
CERTIFICATE NO.
17915
MICHAEL S.
MAMLOUK
Date Signed 12/16/88
ARIZONA, U.S.A.

17. Key Words

Overlay Design, Flexible Pavement, Roughness, Fatigue, Plastic Deformation, Nondestructive Testing, Deflection, Resilient Modulus, Dynamic Analysis, Backcalculation, Stress Sensitivity, Economic Analysis

18. Distribution Statement

Document is available to the U.S. public through the National Technical Information Service, Springfield, Virginia 22161

19. Security Classification (of this report)	20. Security Classification (of this page)	21. No. of Pages	22. Price
Unclassified	Unclassified	234	

ACKNOWLEDGEMENTS

The authors would like to thank many people who contributed to the success of this project. Special thanks go to the ADOT personnel who provided valuable input and assistance during the course of the project. These people include:

Mr. Frank R. McCullaugh
Mr. Larry Scofield
Mr. Richard Power
Mr. Steven L. Tritsch
Dr. Subodh Kumar
Mr. George B. Way
Mr. James Delton
Mr. Gary L. Cooper
Mr. John F. Eisenberg
Mr. John E. Lawson

The authors appreciate the cooperation and important input from all of the ADOT personnel.

The principal investigator of this project is Dr. Michael S. Mamlouk and the co-principal investigators are Drs. William N. Houston, Sandra L. Houston and John P. Zaniewski. Two research assistants participated in this project especially in the laboratory testing, data collection and data analysis. These research assistants are Messrs. Rohan W. S. Perera and Tim Anderson. The field sample collection and cone penetration testing were performed by Foree and Vann, Inc. The nondestructive testing was performed by ADOT personnel and ERES Consultants, Inc. R-value tests were performed by ADOT.

VOLUME I

TABLE OF CONTENTS

LIST OF TABLES

LIST OF FIGURES

TECHNICAL SUMMARY

A large percentage of highway budget in Arizona is being devoted to upgrading and maintaining existing roads. A mechanistically-based overlay design method was needed in order for the rehabilitation process to be performed in a more optimal manner. In this study, a rational overlay design method for flexible pavements in Arizona has been developed which considers roughness, fatigue and plastic deformation failure criteria. The method is also capable of analyzing the economics of overlay projects and other rehabilitation alternatives.

During the development of the method, twenty in-service pavement sites were selected from various locations in Arizona for detailed evaluation and data collection. Several factors were considered during the selection of these sites including the availability of historical records and the representation of various geographical and environmental regions, soil types, pavement conditions and traffic volumes. At each site a total of 10 stations were established at a spacing of 10 ft apart. These stations were located in the right-hand wheel track of the right lane. Station 1 was set at a distance of 1 ft ahead of the milepost marker corresponding to the site.

Nondestructive tests (NDT) were performed using the Dynaflect and the Falling Weight Deflectometer (FWD) at the ten stations at each site. The FWD was operated at 3 stress levels (6, 9 and 12 kips) at stations 1, 5 and 10 at each site, while one stress level at 9 kips was used at the other stations. All 20 sites were tested with the FWD, while sites 1 through 13 and 15 were tested using the Dynaflect.

In order to more accurately determine the subsurface profile, and to detect layering, cone penetration testing (CPT) was performed at three locations at each test site. In general, these locations correspond to station 1, the shoulder adjacent to station 1 and station 4. The CPT followed the ASTM D3441-86 procedure to depths of 25 ft or refusal.

Asphalt concrete cores, base and subbase samples and undisturbed subgrade samples were collected from the 20 test sites. Unless otherwise noted, the boring locations were at stations 1, 4 and 7 at each site. Resilient modulus tests were performed in the lab on asphalt concrete cores at three temperatures according to ASTM D4123-82 procedure. In addition, resilient modulus tests were performed in the lab on the undistrubed subgrade materials according to AASHTO T274-82 procedure with some minor modifications. Moreover, base and subbase gradation as welll as subgrade soil classification and Atterberg limits were obtained. One cement treated base sample was also tested for resilient modulus.

The study concluded that the variability of NDT data across a 90 ft span can be attributed primarily to spacial variability in material properties. It was also found that within the stress range of the FWD tests (6 to 12 kips), the effect of material nonlinearity was less significant than the effect of spacial variability in material properties. However, at stress levels associated with the Dynaflect, there may be a more significant effect of material nonlinearity when compared with FWD stress levels.

The CPT results showed that there is a large number of distinct layers within the subgrade resullting in a wide variation in subgrade stiffnesses in the first 25 ft.

The layer moduli were manually backcalculated using both Dynaflect and FWD data. Both static and dynamic analyses were used for this purpose. The asphalt concrete modulus was further adjusted to a reference temperature of 77°F for the purpose of comparison with the lab moduli and to 70°F for the purpose of developing the overlay design method. The difference between the results of static and dynamic analyses was found to be moderately small. Although the dynamic analysis results (considering the inertial forces) are considered to be more accurate, the differences are too smalll to justify the greater complexities and time requirements of dynamic analyses for routine design computations. An automated computerized backcalculation procedure using static analysis has been developed for use in design.

The backcalculated moduli were compared with lab-measured moduli. On the average, the lab-measured asphalt concrete moduli were about three times as high as the backcalculated values, with significant deviations from the average. However, the backcalculated subgrade moduli were about 50 percent higher than the lab values, with significant deviations from the average. A number of factors which might contribute to these differences were presented and discussed. It was concluded that the major contributor to these differences is that the lab moduli represent only the small specimens on which the tests were performed, while the backcalculated moduli from NDT are weighted-average values representing relatively large volumes of material. For most overlay design procedures, the NDT values would be more useful.

For the purpose of developing an overlay design procedure, three failure criteria were used; roughness, fatigue and plastic deformation. The roughness model was developed using the ADOT data base. The Maysmeter roughness before overlay was correlated with the roughness after overlay. Also, the rate of change of roughness was found to be well correlated with time, but it was poorly correlated with overlay thickness, layer moduli, traffic loading and regional factor. Thus, knowing the roughness before overlay the time before reaching the roughness failure level can be computed.

The fatigue model was developed through consideration of fatigue curves from the literature and from data from Arizona highways. The fatigue model is based on the cumulative damage concept (Minor's law). It relates the number of load applications to the tensile strain at the boottom of AC layer. The fatigue curve selected for Arizona pavements indicates that they are somewhat more resistant to fatigue failure than other pavements. Using the fatigue model the overlay thickness required to protect the pavement from fatigue cracking during the design period can be computed.

The plastic deformation model was developed to insure that the overlay thickness is adequate for protection against excessive plastic deformation. The model is based on FWD testing at different stress levels.

The three pavement failure criteria (roughness, fatigue and plastic deformation) were incorporated in an integrated CART (Center for Advanced Research in Transportation) Overlay Design for Arizona (CODA). A microcomputer program CODA was also developed to compute the required overlay thickness as well as performing economic analysis for various rehabilitation procedures. The CODA procedure is recommended for implementation by ADOT for future overlay designs.

CONVERSION FACTORS, U. S. CUSTOMARY TO METRIC (SI) UNITS OF MEASUREMENT

U. S. customary units of measurement used in this report can be converted to metric (SI) units as follows:

Multiply	By	To Obtain
inches	2.54	centimetres
feet	0.3048	metres
miles (U. S. statute)	1.609344	kilometres
pounds (mass)	0.4535924	kilograms
pounds (force)	4.448222	newtons
pounds (mass) per cubic foot	16.0185	kilograms per cubic metre
pounds (force) per square inch	6894.757	pascals
kips (force)	4448.222	newtons
kips (force) per square inch	6.894757	megapascals
Fahrenheit degrees	5/9	Celsius degrees or Kelvins*

* To obtain Celsius (C) temperature readings from Fahrenheit (F) readings, use the following formula: $C = (5/9)(F - 32)$. To obtain Kelvin (K) readings, use: $K = (5/9)(F - 32) + 273.15$.

CHAPTER 1. INTRODUCTION

1.1. PROBLEM STATEMENT

For a variety of reasons, the number of new highway construction projects is steadily decreasing. As a consequence, a higher percentage of resources is being devoted to upgrading and maintaining existing highways. Thus, overlay design has moved into the forefront of highway engineering.

The primary goal in overlay design is to provide a section which can withstand the applied traffic loads throughout the design life without pavement failure such as excessive cracking, rutting or loss in serviceabililty. Fundamental engineering decisions include assessing which sections of highway require overlaying and how much overlay is needed.

The lack of basic research in the pavement area for the past few decades has hampered the development of new knowledge on pavement behavior. New mechanistically-based design methods should be developed to close the gap between theory and practice and to upgrade the performance of the existing highway system. As a part of this study, detailed consideration has been given to basing overlay design on a more rational analysis of nondestructive testing data as well as on typical pavement performance in Arizona.

The loads applied by traffic and by most deflection measurement devices on pavement structures are dynamic in nature. When truck wheels impact the pavement, it is subjected to a series of half sine waves. The duration of the wave pulse could be dependent on the speed of the moving wheel and the depth in the pavement system at which the response is analyzed.

Deflection measurement devices have been extensively used in the past few decades to evaluate the load-deformation response and the overlay design of highway and airfield pavement systems. One of the earliest devices developed for this purpose was the Benkelman Beam. Because of the static loading condition, generation of creep in the pavement, and the slow operating rate, the Benkelman Beam is outdated. Vibratory deflection measurement devices such as the Dynaflect, Road Rater and the 16-kip Vibrator developed by the U.S. Army Waterways Experiment Station, were developed for better characterization of pavement properties. The vibratory devices apply dynamic loads, and surface deflections are measured at several lateral distances, however, these devices do not accurately simulate loads applied by moving vehicles. More sophisticated deflection measurement devices were developed, such as the Falling Weight Deflectometer (FWD) and the FHWA Thumper, that better simulate moving wheel loads. Currently, highway and airfield agencies are moving towards using the FWD and reducing dependence on other devices.

The technology is available to utilize nondestructive measurement devices that accurately simulate actual traffic conditions. The missing link, however, is an acceptable method of analyzing the data. Analysis of data obtained from actual traffic loading and from dynamic loading devices has previously been based on either empirical approaches or static (elasto-static and viscoelasto-static) models. Empirical correlations are restricted to conditions similar to those from which they were originally developed, while static analyses neglect the inertia of the pavement. Most computer programs currently used in analyzing pavement response are based on static analyses.

In other words, it is assumed that the dynamic response of pavement structures is not different from the static response. In fact, the static and dynamic responses of pavements may be significantly different. Field data show that pavement response is dependent on mode of loading and/or load frequency, a condition which cannot be interpreted using any static analysis. For example, Figures 1-1 and 1-2 show that deflection devices with different modes of loading generate slightly different responses on the same pavement sections, even after the data are normalized to the same force level. These differences are no doubt due in part to differences in dynamic response and in part to stress level sensitivity.

In addition, the subgrade moduli obtained through analysis of deflection measurements have not been verified under different loading conditions, especially in Arizona. Since the deflections at the pavement surface are sensitive to various layer moduli, any improvement in the accuracy of the subgrade modulus would increase the confidence in the remaining moduli. Therefore, independent methods of modulus measurement such as lab testing and cone penetration testing, when compared to the calculated moduli from deflection measurements, may provide some new insight into the best method for evaluating the subgrade modulus. If a substantial improvement in measuring moduli can be made, then a corresponding improvement in overlay design procedures can be made.

1.2. OBJECTIVES AND SCOPE OF WORK

The overall objective of this study is to improve pavement overlay design procedures for the Arizona Department of Transportation.

The overall objective has been pursued by accomplishing a series of intermediate objectives as follows:

1. Improved material characterization by
   a) Developing better techniques for analyzing NDT data. This was accomplished by developing an improved backcalculation procedure and evaluating the importance of the dynamic response of pavements under various loading conditions, as compared to static.
   b) Adding to the existing material characterization data base by performing laboratory triaxial resilient modulus testing on subgrade materials from Arizona pavements
   c) Adding to existing material characterization data base by performing laboratory resilient modulus testing on asphalt concrete cores from Arizona pavements.
   d) Adding to existing material characterization data base by performing cone penetration testing on subgrade materials from Arizona pavements.

2. Evaluation of non-linear subgrade response on overlay design parameters.

3. Assessing variability in pavement section properties across a particular pavement "site." This was accomplished by evaluating

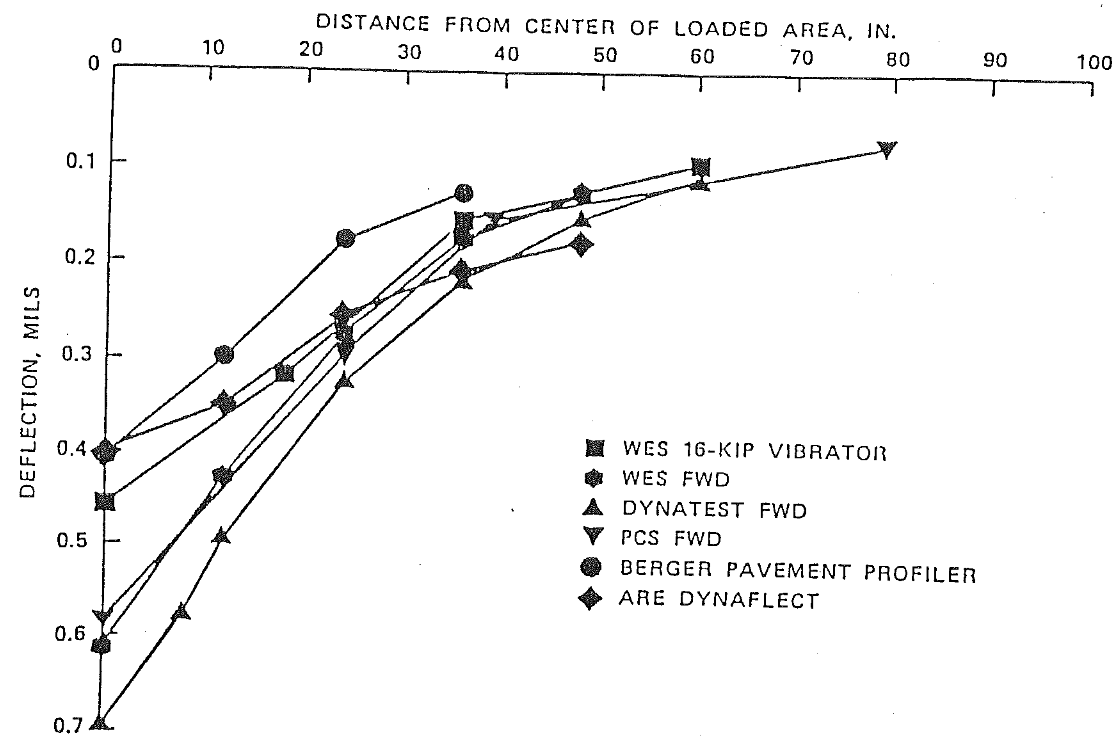

FIGURE 1-1. DEFLECTION MEASUREMENTS OF FIVE NDT DEVICES ON A FLEXIBLE PAVEMENT NORMALIZED TO 1000-LB FORCE LEVEL (1)

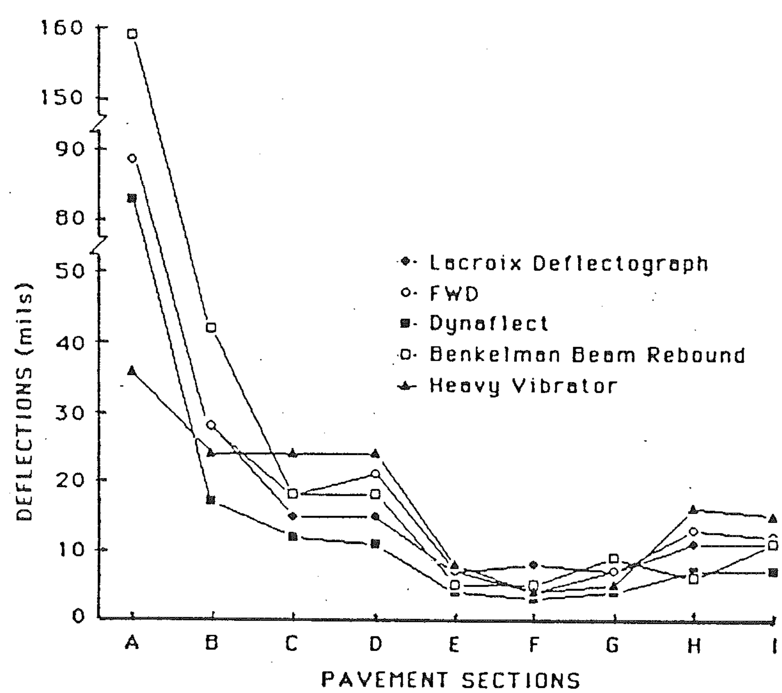

FIGURE 1-2. COMPARISON OF DIFFERENT MEASUREMENT METHODS ON DIFFERENT ROAD STRUCTURES, WITH DEFLECTIONS NORMALIZED TO 11,250-LB LOAD (2)

the means, standard deviations, and coefficients of variation for surface deflection measurements taken over a 90 ft stretch of highway.

4. Evaluating the performance of Arizona pavements using the available pavement management data base, and developing a rational overlay design method for Arizona. Three design models were developed; roughness, fatigue and plastic deformation.

5. Developing an economic analysis technique to compare the costs of several rehabilitation options such as overlay only, milling plus overlay, milling, recycling plus overlay, and reconstruction. The results of these accomplishments are presented in this final report.

CHAPTER 2. LITERATURE REVIEW

2.1. BASIC OVERLAY DESIGN APPROACHES

The most commonly used overlay design procedures are: a) engineering judgment b) standard thicknesses c) empirical and d) mechanistic or mechanistic-empirical. A brief description of these procedures is discussed in the following paragraphs (3).

2.1.1. Engineering Judgment - This approach is based on previous experience; in many ways, it is still a part of most current overlay design procedures. The advantage of this procedure is the direct tie between the design and the experience of the engineer, which usually guarantees the design will not be grossly inconsistent with experience. The disadvantage is that the experience available may not cover the design requirement at hand. Furthermore, methods based almost entirely on engineering judgment may not be sufficiently sophisticated and detailed to account for variations in the numerous factors which influence overlaid pavement performance.

2.1.2. Standard Thicknesses - Some agencies use this procedure, either formally through policies, or informally. For a given existing pavement type, traffic level, pavement thickness and other factors, a standard overlay thickness is prescribed.

2.1.3. Empirical - The degree of empiricism varies from one design method to another. Basically, relationships are developed between performance of overlay thicknesses and known data such as age, traffic, construction, structural section, and environmental factors. Regression techniques are normally used to develop such relationships. Deflection measurements are commonly used to characterize the structural adequacy of the pavement sections before overlay. The basic concept of these deflection-based analyses is that similar pavements with higher deflections will fail more quickly than those with lower deflections under the same loading. This approach has gained wide acceptance and is currently used by many states.

2.1.4. Mechanistic or Mechanistic-Empirical - Mechanistic design procedures differ from others in that they are used to characterize the response of the pavement to a load in terms of basic parameters such as strains or stresses. On the other hand, failure is normally defined in terms of specific mechanisms such as fatigue cracking and/or rutting. For the system to be fully mechanistic, fracture mechanics should be used to determine the relation between strain or stress and cracking, and basic mechanical and theoretical concepts should be used to determine the relation between stresses and permanent deformation. Also, the response of the pavement to dynamic loading should be correctly analyzed, using an appropriate method of analysis.

Currently, no completely mechanistically-based overlay design method exists. All mechanistically-based methods depend in part on empirical relations between pavement parameters and the number of load applications the pavement can support before failure. For example, the strain at the bottom of the existing asphalt layer is normally correlated to fatigue damage to develop a fatigue failure criterion. In some instances, the stress or strain at the top of the subgrade has also been correlated to rutting resulting in a permanent deformation failure criterion.

All existing mechanistically-based methods of overlay design use static analyses to determine the dynamic response of the pavement structure. Recent studies (4-16) indicate the dynamic response of pavements may be different from the static response. Therefore, if the available static multilayer elastic computer programs (such as Chevron, ELSYM5, BISAR, VESYS, BISTRO, ILLI-PAV, etc.) are used to predict the response of pavements, the results may be misleading due to the inability of these programs to model the dynamic characteristics of pavement loading. On the other hand, if the dynamic analysis does not significantly affect the required overlay thickness, a simpler static analysis would be preferred. Thus, both advantages and disadvantages of the dynamic analysis need to be evaluated and a decision has to be made as to which type of analysis to consider in the overlay design process.

In addition, when a condition survey or other considerations indicate a need for an overlay, a set of deflection measurements would be taken at enough locations to statistically characterize the section to be overlaid. The deflections imposed would be less than or equal to the maximum deflection previously imposed thousands of times by traffic. Thus, the strains imposed during the surface deflection measurements would be expected to be essentially elastic, due to the conditioning of the pavement layers and subgrade by the traffic.

Although the strains imposed by loading, for measurement purposes, would be expected to be elastic, they may be non-linear. Indications from the literature review are that there may be some nonlinearity in the response of pavement materials (17-21). The effect of material nonlinearity is not taken into account in most of the available multi-layer elastic computer programs. If the non-linearity is significant, then moduli back-calculated from light vibrators, such as the Dynaflect, could be significantly different from those obtained from a heavy load device, such as the Falling Weight Deflectometer.

The major advantage of the mechanistically-based approach, even when empirical relations between calculated strain or stress and number of applications to failure are used, is that the overlay requirements can be determined for any pavement for which the strain and stress can be calculated. Users are not limited to pavements with which they have extensive experience; instead, they can analyze the expected performance of new designs and the influence of new materials. Another significant advantage of this approach is that past and projected damage can be calculated more accurately. In some environments, there are significantly different subgrade support conditions throughout the year, affecting the stress or strain in the pavement. A mechanistic procedure will allow damage in various seasons of the year to be calculated and used in the analysis.

The Arizona Department of Transportation (ADOT) is actively engaged in the design and construction of pavement overlays. ADOT reports (22,23) describe a recently developed overlay design procedure called Structural Overlay Design for Arizona (SODA). The first version of the method is essentially deflection-based utilizing the Dynaflect (a light vibrator) measurements. The procedure was developed from both theoretical analyses and considerable field data. It is based heavily on data from actual Arizona pavement materials and it employs most of the parameters that regression analyses indicate are important to performance such as traffic load regional factor, roughness, spreadability index, and the number 5 Dynaflect sensor reading. Other parameters such as layer thicknesses and moduli were not included in the SODA equation since regression analyses proved that they are insignificant.

The SODA method uses as input values:

1) Total traffic loads expected over the design period (18 kip equivalents).
2) Road roughness (Mays-meter value)
3) Regional Factor
4) Spreadability Index = ((sum of the 5 sensor readings)/(5x#1 sensor)) x 100 based on Dynaflect tests.
5) Dynaflect #5 sensor readings

The equation for thickness is:

$$T = \frac{\text{Log } L + 0.104 \times R + 0.000578 \times Po - 0.0653 \times SIB}{0.0587 \times (2.6 + 32.0 \times D5)^{0.333}}$$

Where:

L = 18k loads in 1000's
R = Regional Factor
Po = Roughness, inches/mile
SIB = Spreadability index before Overlay
D5 = #5 Dynaflect sensor reading.

The overlay thickness should be determined at each test location and the mean value of thickness for all test locations in a design section is then used as the overlay thickness. No statistical manipulations are needed as they were incorporated into the development of the method. Any individual test location results less than zero are assigned a value of zero, and any results over 6 inches are assigned a value of 6 inches.

The developers of the method state that the method still needs some improvements. One potential shortcoming is that it is based on small deflections from a light vibrator. Thus, if FWD data are incorporated in the design procedure, the method can be improved. Also, if dynamic analyses and material non-linearities have a significant impact on overlay design, some modification to SODA may be warranted. Furthermore, incorporating more of the material properties parameters such as the layer moduli or providing better estimation of critical stresses or strains in the pavement structure might improve the method.

The SODA method was later modified by ADOT to use FWD measurements. The modification was essentially performed using regression analyses between Dynaflect and FWD data. It should be noted that the use of regression analysis in the original development of the method is associated with a certain degree of error. Further use of regression analysis to transfer from

Dynaflect data to FWD data increases the error associated with the use of the method.

The research performed herein is aimed at developing a rational overlay design procedure considering roughness, fatigue and plastic deformation criteria. The significance of dynamic analysis and the effect of nonlinearity are evaluated. Finally, a comparison between the results of the new overlay method and the SODA method is to be evaluated.

2.2. FACTORS CONSIDERED IN OVERLAY DESIGN

The literature includes a number of overlay design methods based on deflection measurements (24). Most of these methods have common features and take into consideration the following factors:

1. The season in which testing is performed.
2. The location on the pavement where tests are made.
3. The frequency of testing along the pavement.
4. The need for taking cores and performing laboratory tests.
5. The NDT device(s) that are or may be used.
6. The measurements that are made with the NDT devices, such as single deflection under the load, peak-to-peak deflections, or deflection basin.
7. The other measurements made in addition to NDT, such as air temperature, pavement temperature, etc.
8. The corrections made either to the NDT measurements or to the calculated pavement properties to consider the temperature and seasonal differences between measurement conditions and design conditions.
9. The properties of the pavement or layers calculated or inferred from the NDT measurements. These properties can be either qualitative ratings, representative basin properties, representative structural properties, or layer moduli.
10. The methods used to distinguish between sections of pavement that require different thicknesses of overlay.
11. Empirical relations used to convert the NDT measurements to design parameters. These conversions may be:

    a. Correlations between the deflections measured with NDT device and those produced by a design load,
    b. Correlations between layer materials properties corresponding to the load level applied by the NDT device and the same material properties at design load level, or
    c. Correlations between an NDT deflection and a design strain at a critical point in the pavement structure.

12. Empirical design relationships that convert the measurement at design load into the number of load applications that the pavement can support.

Specific details about individual overlay design methods are presented in Refs. (25-43).

2.3. CONCEPTS OF DYNAMIC ANALYSIS

The load applied by traffic and most NDT devices is dynamic in nature. When a dynamic load is applied to pavements, the inertia of the vehicle and/or the pavement system may play an important role in the resulting deflections.

When a dynamic load is applied at the surface of a homogeneous media, the energy is transmitted to the ground by a combination of primary (compression), secondary (shear), and surface (Rayleigh) waves. In a layered half-space system such as a pavement structure, multiple wave reflection and refraction occur. The problem is more difficult to analyze than a homogeneous half-space system. Although not seen by eye, the surface waves developed when an impulse load is applied on the pavement are similar to the waves developed on a smooth surface of water when a rock is dropped into it. These waves propagate away from the source of excitation and eventually die due to the damping of the pavement system.

Up to the present, analyses of data (obtained from dynamic loading) which are based on mechanistic approaches use static models. Several multilayer elastic computer programs (such as Chevron, ELSYM5, BISAR, VESYS, BISTRO, ILLI-PAVE, etc.), which are based on static analyses are currently used in analyzing the dynamic response of pavement. Pavement response to dynamic loading may be dependent on the mode of loading and/or frequency. The dynamics of the pavement system can be represented using either single or multiple degree of freedom modeling systems.

2.3.1. Single Degree of Freedom (SDOF) System - In this approach the pavement system is represented by a combination of masses, springs and dashpots (44). Although SDOF models take into account inertial effects, one of their major shortcomings is the assumption that loads, deflections, stresses and strains are applied in one direction; i.e., the vertical direction. In fact, when a vertical load is applied, stresses and strains are developed in all directions throughout the pavement structure. Thus, the SDOF model cannot represent the three dimensional nature of the pavement response. Deflections at points away from the load (at various geophone locations) cannot be predicted.

2.3.2. Multidegree of Freedom System - In this method both the inertial effect and the three-dimensional nature of the pavement structure are considered. Although the effect of inertia has been recognized for a long time, no three-dimensional dynamic solution was available for multilayer elastic systems until 1982, due to the complicated nature of the problem.

The load applied by the moving wheels of trucks and airplanes on pavements can be represented by a series of half sine waves. The magnitude and duration of such waves depend mainly on the magnitude of the applied load, the speed of the vehicle and the depth in the pavement system at which the effect is considered. To simplify the analysis, the wave (transient) mode of loading can be represented by a series of harmonic loadings having different frequencies and magnitudes. The transformation from transient to harmonic loadings can be easily performed using Fourier transformation. Therefore, once the pavement response to harmonic loading, as a function of frequency and magnitude, is evaluated, the response to any wave (transient) mode of loading can be obtained.

The governing equation for steady-state (harmonic) elastodynamics is the Helmholtz equation (45), written in a tensor form as:

$$\mu u_{i,jj} + (\lambda + \mu)\, u_{j,ij} + \rho\omega^2 u_i = 0 \qquad (2\text{-}1)$$

in which λ, μ = Lame's constants; ρ = mass density; ω = circular frequency of excitation; and u_i = i-th cartesian component of the displacement vector. In Equation 2-1, cartesian indicial notation is used in which the subscripts range from 1-3, addition is implied over repeated subscripts, and a comma denotes differentiation with respect to the space variable, i.e., $u_{i,j} = \partial u_i / \partial x_j$. Thus, this tensor form differential equation is a short representation of a number of regular differential equations. The displacement is also assumed to be time harmonic.

The dynamic analysis currently used employ the assumption that the pavement system consists of several layers which are unbounded laterally, but are underlain by a rigid bedrock layer at a finite depth. Full interface bonding (no slip) condition is assumed at the layer interfaces. Materials are assumed to be homogeneous and isotropic, and exhibit either linear elastic or viscoelastic response. A uniformly distributed harmonic circular load is considered to be applied to the pavement surface. A typical multilayered pavement system subjected to dynamic loading is illustrated in Figure 2-1, where each layer is characterized by thickness H, modulus E, Poisson's ratio ν, density ρ, and damping β.

Displacement Computation - The solution of Equation 2-1 for a point load on a half-space is available. However, no closed form solution is available for excitation of layered systems. Therefore, solutions must be obtained by numerical means. Kausel and Peek (46) have recently proposed a numerical technique which renders the elasto-dynamic problem of multilayered systems tractable. The solution is based on the assumption that the displacement field is linear in the direction of layering between adjacent interfaces. Thus, sufficiently thin layers must be specified to ensure the validity of this representation. In practice, artificial sublayers may be introduced in order to satisfy this requirement.

Finally, the response of the pavement system to the wave (transient) mode of loading can be obtained by adding the responses due to a number of harmonic loadings using Fourier transformation as indicated earlier. Using this procedure, the in-phase and out-of-phase deflections in the vertical, radial and tangential directions at any point in the pavement system can be computed.

Stress and Strain Computation - Once the deformations in the vertical, radial and tangential directions are determined, the normal strains can be calculated using the theory of elasticity as follows.

$$\varepsilon_z = \frac{\partial \omega}{\partial z}$$

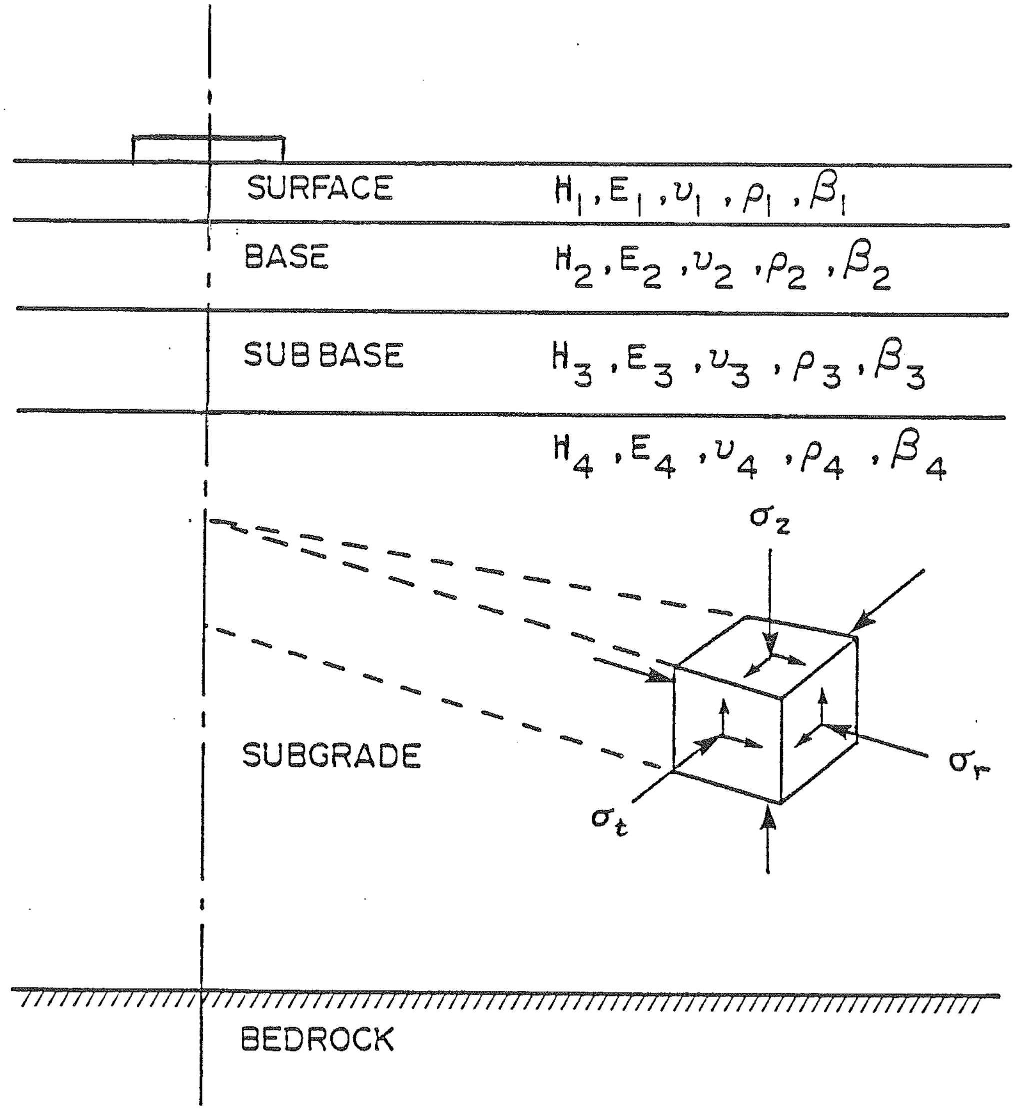

FIGURE 2-1. TYPICAL MULTILAYERED PAVEMENT SYSTEM SUBJECTED TO DYNAMIC LOAD

$$\varepsilon_r = \frac{\partial u}{\partial r}$$

$$\varepsilon_t = \frac{u}{r} + \frac{\partial v}{\partial \theta} \qquad (2\text{-}2)$$

where ε_z, ε_r, and ε_t are the vertical, radial, and tangential strains, respectively; ω, u, and v are the vertical, radial, and tangential displacements, rpspectively; and z, r, and θ are the vertical, radial, and angular coordinates, respectively.

The displacements can not be obtained using a closed form solution. The differentiation can be carried out using a numerical approach, such as the finite difference solution. In addition to the normal strains, the shear strains can also be computed using similar procedures. The normal and shear stresses can then be computed from the theory of elasticity using the generalized Hooke's law. Further details about the theory of dynamic analysis are presented in Reference 11.

It should be noted that the subject of dynamic analysis can be divided into two areas. The first area, which can be referred to as vehicle dynamics, deals with analyzing the dynamic loading of vehicles due to pavement roughness and the truck suspension system (14-16). The second area, which can be referred to as pavement dynamics, deals with analyzing the dynamic response of pavements due to vehicle dynamic loading (4-13). The two areas are complimentary. The ultimate goal is to study the interaction between vehicle dynamic loading and the pavement dynamic response. Up to the present time, this interaction effect has not been reported in the literature.

Results from experimental research performed on in-service pavements (1,2,47-49) indicate some differences in pavement response under various modes of loading (static, harmonic and transient) and under various frequencies of harmonic loading.

The dynamic solution of multi-layered elastic systems was incorporated in a computer program by Kausel (46). This version of the dynamic program is capable of computing the in-phase and out-of-phase vertical, radial, and tangential displacements at any point in the multi-layer system (due to harmonic loading). The program was further modified by Sebaaly (11) to compute stresses and strains, in addition to displacements, caused by harmonic and impulsive loadings. The currently available programs are:

1. DYNAMIC1, which computes the response of multi-layered systems to harmonic loading
2. DYNAMIC2, which computes the response of multi-layered systems to impulsive loading
3. DYNAMIC3, which back-calculates the layer moduli of multi-layer systems if the deflections due to harmonic loading are known.

The DYNAMIC1 and DYNAMIC2 programs are capable of handling pavements with any number of layers within the capability of the computer memory. The static response can also be obtained by assuming a loading frequency of zero in DYNAMIC1 or a very long load duration in DYNAMIC2. The static response was checked against Chevron program for similar conditions and loading, and identical results were obtained.

The DYNAMIC3 program was developed in this study in order to backcalculate the layer moduli, given deflections due to harmonic loading. During the development of this program, the concepts of DYNAMIC1 and CHEVDEF (50) programs were used. The program is capable of handling up to 4 layers, including the subgrade.

The current version of DYNAMIC1, DYNAMIC2 and DYNAMIC3 programs are used with the VAX-VMS mainframe computers. Their operation requires several minutes of running time, depending on the number of layers and the number of output parameters required. No microcomputer version of these programs is currently available. The DYNAMIC1, DYNAMIC2 AND DYNAMIC3 programs, together with flow charts and user's guides, were previously submitted to ADOT.

2.4. MATERIAL AND SYSTEM PROPERTIES

Material properties used in the mechanistic analysis of a multilayer pavement system are elastic moduli (Young's moduli, shear moduli, etc.), Poisson's ratios, mass densities, and material damping ratio. A brief discussion of some of the material and pavement system properties as they relate to dynamic analysis are presented below.

2.4.1. Layer Moduli - The stress-strain relations of isotropic elastic materials are, in classical formulations, expressed in terms of fundamental material parameters, e.g., Young's modulus, and Poisson's ratio. For flexible pavement materials, however, it has become common to define state dependent parameters such as the resilient modulus and the dynamic modulus. These parameters are often used to interpret the nonlinear and time-dependent response of pavement materials. The resilient modulus is obtained by subjecting a specimen to repeated stresses and measuring the recoverable strain after a number of load applications, as shown in Figure 2-2. The resilient modulus, therefore, is the Young's modulus of the material after many load repetitions, i.e., the "shake-down modulus" of the material, which is normally different from the initial value. On the other hand, the dynamic modulus is obtained by subjecting a finite specimen to harmonic loading and determining the ratio of the stress amplitude to the corresponding strain amplitude, as illustrated by Figure 2-3.

Clearly, the resilient modulus is relevant to the analyses of pavement deflections since field deflection data reflect the current stiffness of pavements. The dynamic modulus, however, can be used only if the phase lag between load and deformation is also considered (complex modulus). Laboratory measured values of complex moduli obtained from the dynamic modulus test can yield valuable information on the fundamental material parameters such as stiffness and internal damping, provided that these tests are properly interpreted. Such data, combined with a rigorous elastodynamic analysis of the pavement structure, offer the greatest promise for progress in evaluating the response of pavements to moving loads.

The "inverse" problem of determining moduli from the response of the pavement structure to surface loading (from NDT devices) has not been fully resolved. No direct theoretical solution is available in the literature to

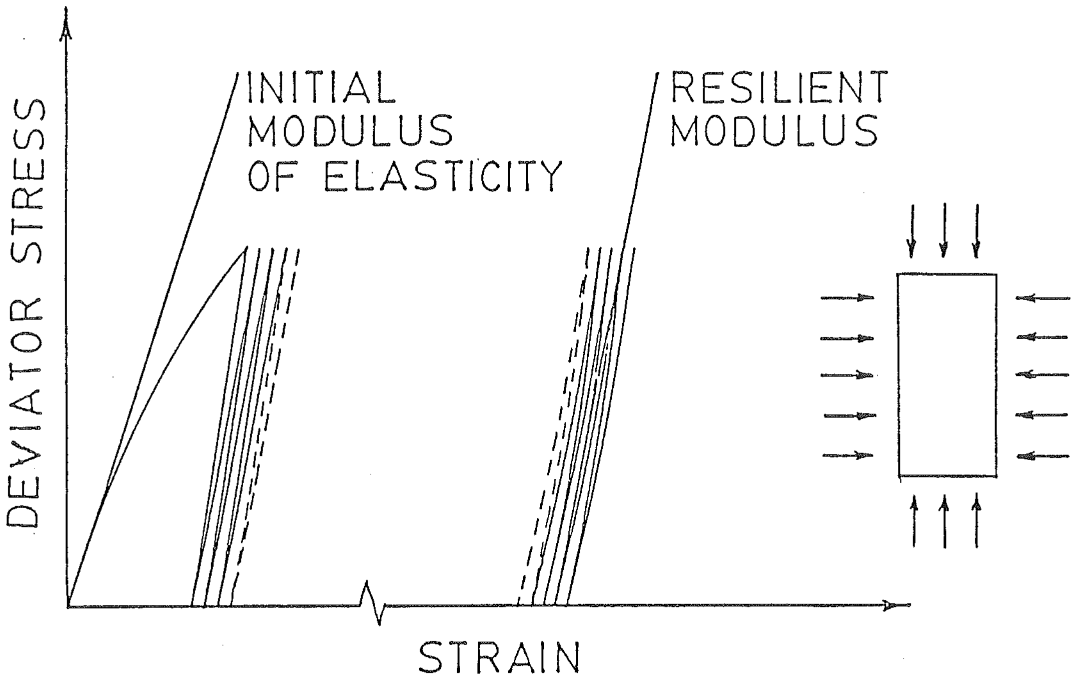

FIGURE 2-2. DEFINITION OF RESILIENT MODULUS

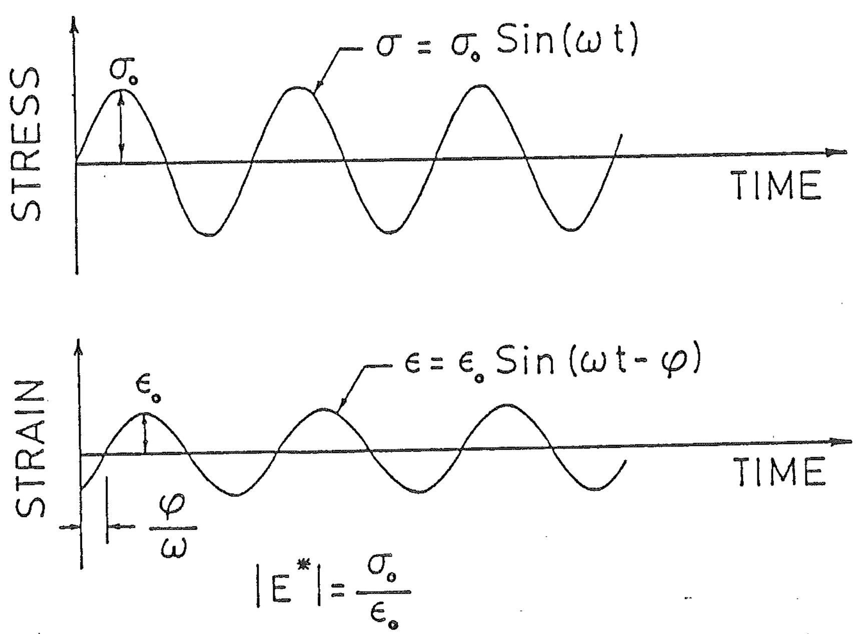

FIGURE 2-3. DEFINITION OF DYNAMIC MODULUS

determine the moduli of a multi-layered system where the surface deflections and layer thicknesses are known. Therefore, it is necessary to employ iterative schemes, that make use of the fact that surface deflections remote from the loaded area are governed primarily by the stiffness of the deeper layers. The predicted moduli are very sensitive to minor changes in surface deflections. Thus, proper procedure has to be followed in order to increase the accuracy of the predicted moduli.

2.4.2. Material Damping - Material damping refers to the internal energy dissipation which occurs in real materials subjected to dynamic loading. Granular pavement materials (gravels, etc.) exhibit hysteretic damping behavior, manifested by a frequency invariant damping ratio with typical values ranging from 2 to 10% (51,52). Using the principle of viscoelasticity, material damping can easily be incorporated into the analysis by replacing Young's modulus by its complex counterpart, i.e.:

$$E^{*} = E(1 + 2i\beta) \tag{2-3}$$

where

E^{*} = complex modulus
E = Young's modulus

i = $\sqrt{-1}$
β = damping ratio

2.4.3. Geometric Damping - When a dynamic load is applied at the surface of a homogenous half-space, the energy imparted to the ground is transmitted away by a combination of waves. These waves encounter an increasingly larger volume of material as they travel outward; thus, the energy density in each wave decreases with distance from the source. This decrease in energy density or decrease in displacement amplitude is called geometric (radiation) damping (51). In a layered half-space system, such as a pavement system, multiple wave reflection and refraction may occur.

The major component, by far, of energy dissipation in pavements results from geometric damping - the dispersion of energy from the source of excitation to the far field - rather than material damping.

2.4.4. Out-of-Phase Response - If a static load is applied to the pavement system, the pavement response will be in-phase with the load. However, if a dynamic load is applied, the instantaneous pavement response will generally be out-of-phase with the load, due to both geometric and material dampings. In fact, the pavement surface takes a wave form propagating away from the load. Using the Dynaflect sensors, only peak-to-peak surface deflections are recorded and no information is obtained regarding the instantaneous pavement response or the out-of-phase condition as illustrated in Figure 2-4. The dynamic response of the pavement can be represented by a complex number in which the real part represents the in-phase response, while the imaginary part represents the 90° out-of-phase response.

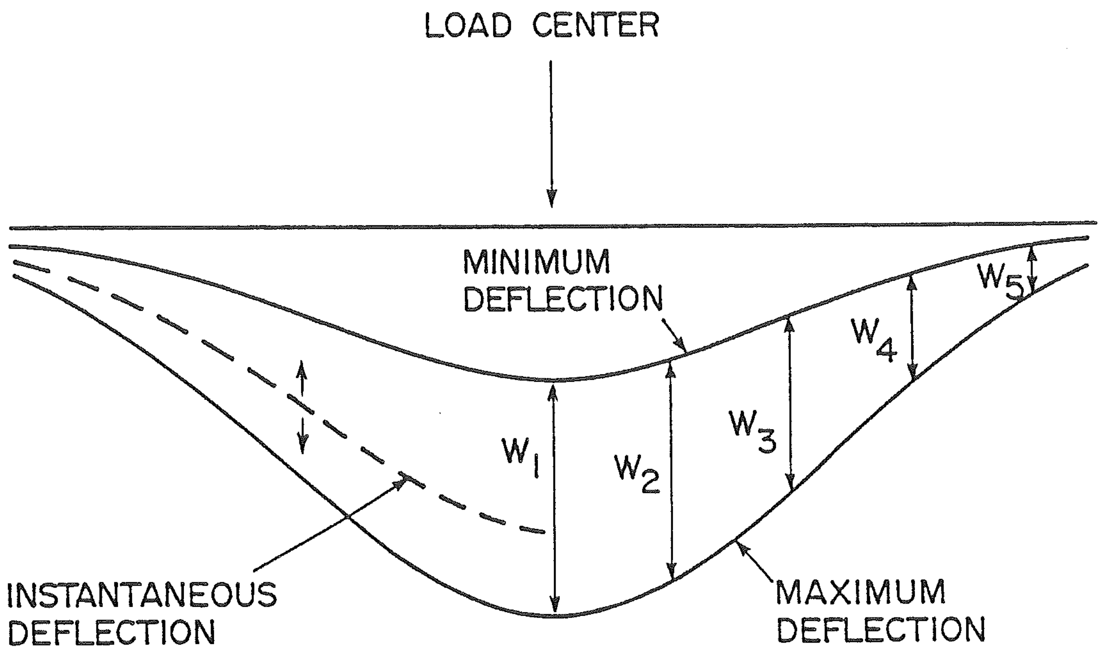

FIGURE 2-4. DEFLECTIONS MEASURED BY THE DYNAFLECT

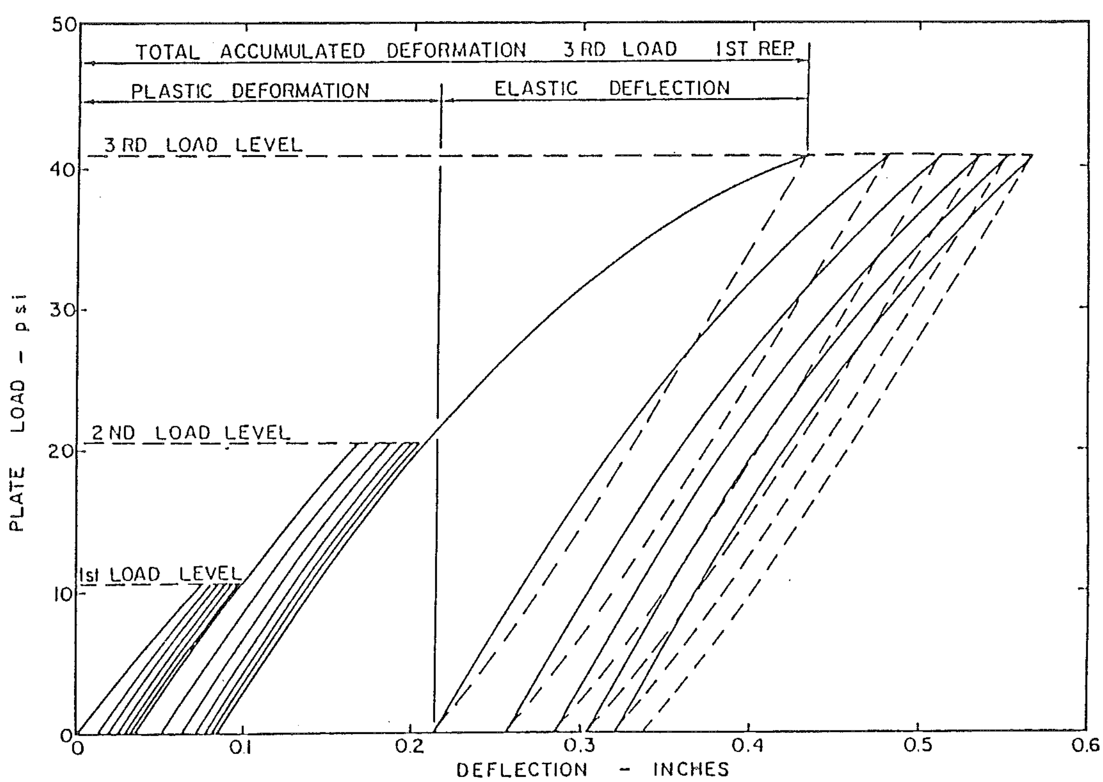

FIGURE 2-5. TYPICAL LOAD DEFLECTION DIAGRAM FROM REPETITIVE PLATE LOAD TESTING (54)

Resonance occurs when the response of the pavement system is 90° out-of-phase with the applied load and, consequently, the applied load is exactly balanced by the damping force (53). The resonant response of the pavement system occurs when the frequency of the applied load equals a natural vibration frequency of the pavement system.

2.4.5. Nonlinearity and Stress Sensitivity - It has long been known that subgrade materials have a nonlinear response to load. However, if the load is repeated several times the effect of nonlinearity is reduced. For example, Figure 2-2 shows a typical stress strain relationship for a soil specimen subjected to a triaxial state of stress where the axial stress is varied in a pulsating form while the confining pressure is kept constant. The nonlinearity is vpry large when the load is applied for the first time. After many applications the response is still somewhat nonlinear, but much less so.

The modulus is affected by the state of stress of the material. For example, the material properties predicted by the light load of the Dynaflect may not be the same as those predicted by a heavy axle load, even if the difference in the mode of loading is considered. As discussed above, the effect of stress sensitivity is reduced when the load is applied several times. Figure 2-5 shows a typical stress-deflection diagram from repetitive plate load testing on a subgrade material according to ASTM test procedure D1195 (54). This figure shows that the peak stress divided by the corresponding recoverable deflection is almost constant regardless of the applied stress level. However, some variation in the tangent moduli still persists after several load applications.

CHAPTER 3. SITE SELECTION

The overall objective of the project is to improve pavement overlay design procedures for ADOT. Pursuant to this objective is the need to improve the materials characterization process and improve performance models. To support this objective 15 pavement sites were originally selected for detailed evaluation during the project, and later they were increased to 20.

The goal of improving pavement performance models required the researchers to concentrate the search for test sites on pavements with good historical records. The Department had performed an evaluation of "Environmental Factor Determination From In-place Temperature and Moisture Measurements Under Arizona Pavements," (55) in 1980. During this study, 37 sites were monitored for five years for temperature, moisture, and deflection. In addition, detailed material sampling and testing were performed. These sites contain the best set of historical data on pavement condition and material properties and therefore, they served as a starting point in the search for test sites for this project.

Given this set of sites, the researchers identified a set of criteria for selection of the 20 sites to be studied as a part of this research:

1. availability of traffic and nondestructive test (NDT) data.
2. availability of material properties such as R-value.
3. overlay history of the site.
4. current pavement condition.
5. geographical distribution.
6. materials in the pavement structure.

All of the 37 sites studied by ADOT met the first two criteria. However, the traffic data for the sites were limited to the data routinely collected by the Department. The available traffic data includes the current annual volume of 18k equivalent single axle loads (ADL or ESAL) and a growth factor. The growth factor is the percent change between the current ADL and the preceeding count. When the rate of traffic growth is nonlinear over time, the data maintained by the Department does not provide an accurate count of the total truck traffic.

Since one objective of the evaluation of the pavement sites was to permit the evaluation or development of performance models for overlaid pavements, criteria number 3 was very important. The most desirable pavement site would be one that had been overlaid one time and the overlay was near the end of its service life. Sites which meet this criteria would provide direct data on the service life of overlaid pavements in Arizona. Unfortunately, only two of the 37 pavements in the data base met this criteria.

Since an insufficient number of sites met the above criteria, the criteria for the present condition of the pavements were established. Distressed pavement sites were sought from pavement sections other than those studied in Reference 55. Unless the pavements were showing distress, the life of the pavements could not be established. The locations of the 20 selected sites are shown in Figure 3-1.

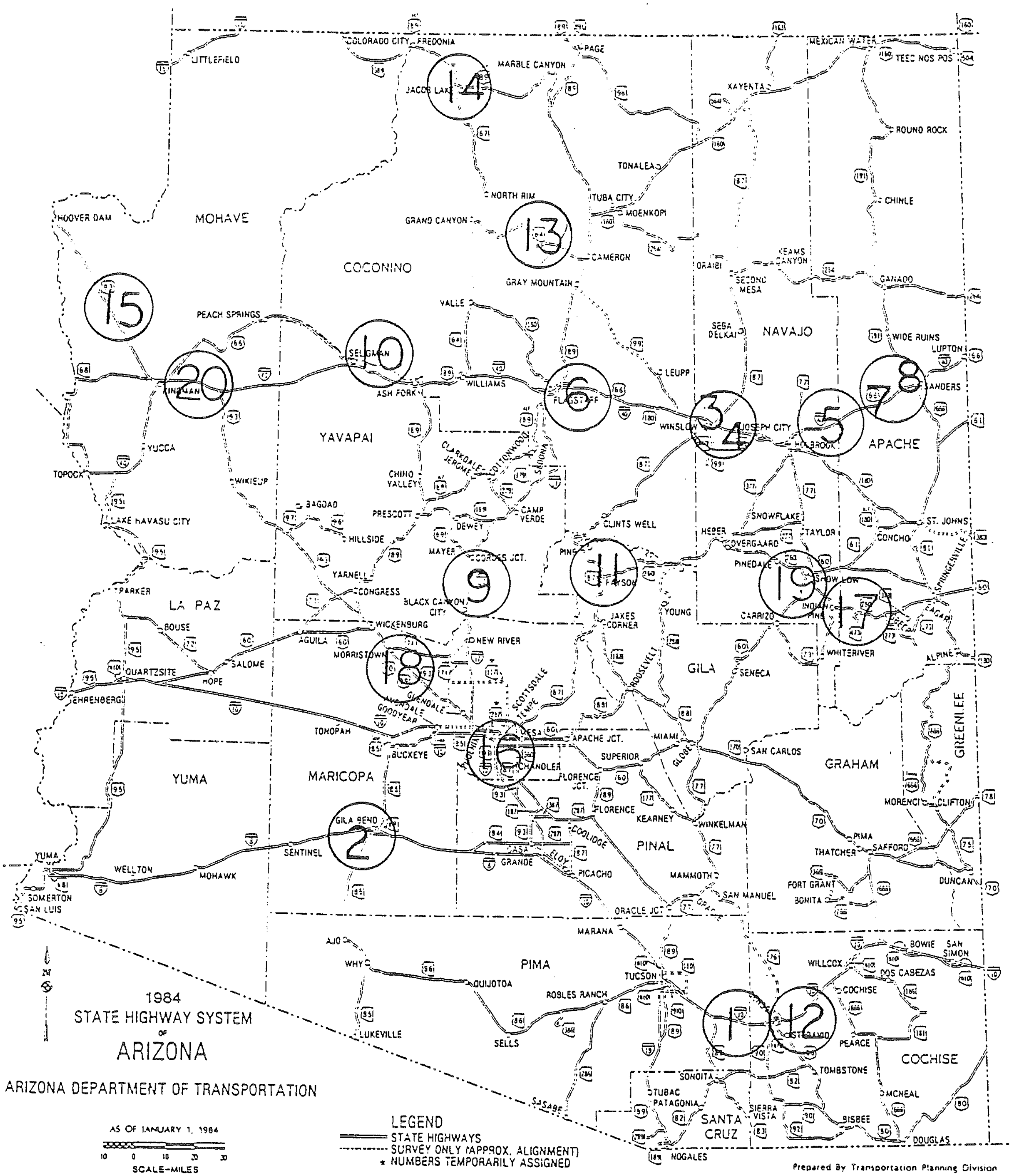

FIGURE 3-1. SELECTED SITES

During the selection process, geographical distribution was an important concern for ensuring the entire range of geographical and climatic conditions were included in the data base. Previous work by the Department identified nine climatic zones in the state as shown in Figure 3-2. Sites were located in eight of the nine climatic zones; zone 5 was not represented. Due to other considerations, various climatic zones were not equally represented. The location of the sites and the climatic zones are given in Table 3-1.

It should be noted that the search for sites did not identify 20 sites which completely matched the criteria, therefore, as will be subsequently discussed, the selection was based on satisfying most of the criteria.

The performance of the sites, as listed in the ADOT pavement management data base, are given in Tables 3-2, 3-3, and 3-4 for cracking, roughness, and friction number respectively. Table 3-5 presents the traffic data, annual truck loads, the traffic growth factor, the maintenance cost in 1986, and the most recent construction project. The data in these tables are for the milepost closest to the site rather than for the actual pavement site.

Review of Table 3-1 shows the sites selected for the research are predominantly on the interstate system. There are two state routes and six U.S. highways, the remaining twelve sites are interstate highways.

Table 3-2 shows ten of the sites had cracking in 1987. Site 15 has the most cracking, 35 percent. Ten of the sites do not have cracking as of the 1987 survey.

Table 3-3 shows the sites have a wide range of roughness. In the ADOT pavement management system roughness less than 165 is considered good and more than 265 is unacceptable. Thirteen of the sites are in the good range, and the remaining sites are in the intermediate category as of 1987. Three sites are close to the unacceptable limit for roughness.

The friction numbers are fairly uniform between the sites, with the exception of Site 9 which has a friction number of 36 as of 1985.

Table 3-5 shows the sites have a wide range of traffic loadings. The ADL ranges from 14 to 2,830 where site 13 has the lowest truck loadings. Table 3-5 also shows site 9 has gone the longest time since a construction project, 1969. The most recent project was on site 5 in 1984. The 1986 maintenance cost data vary widely from zero expenditures on three pavement sites to $22,227 on site 7.

Table 3-6 shows historical construction data for the selected sites, while the abbreviations used are defined in Table 3-7. As shown in Table 3-6, a wide range of material types and layer thicknesses has been represented.

Four of the sites have asphalt-rubber membranes as part of the overlay treatment.

The original surface designs show three sites with a 4" or greater surface thickness, eight sites with an AC layer of less than 4" and nine sites where the original surface was a bituminous stabilized layer. In addition, 2

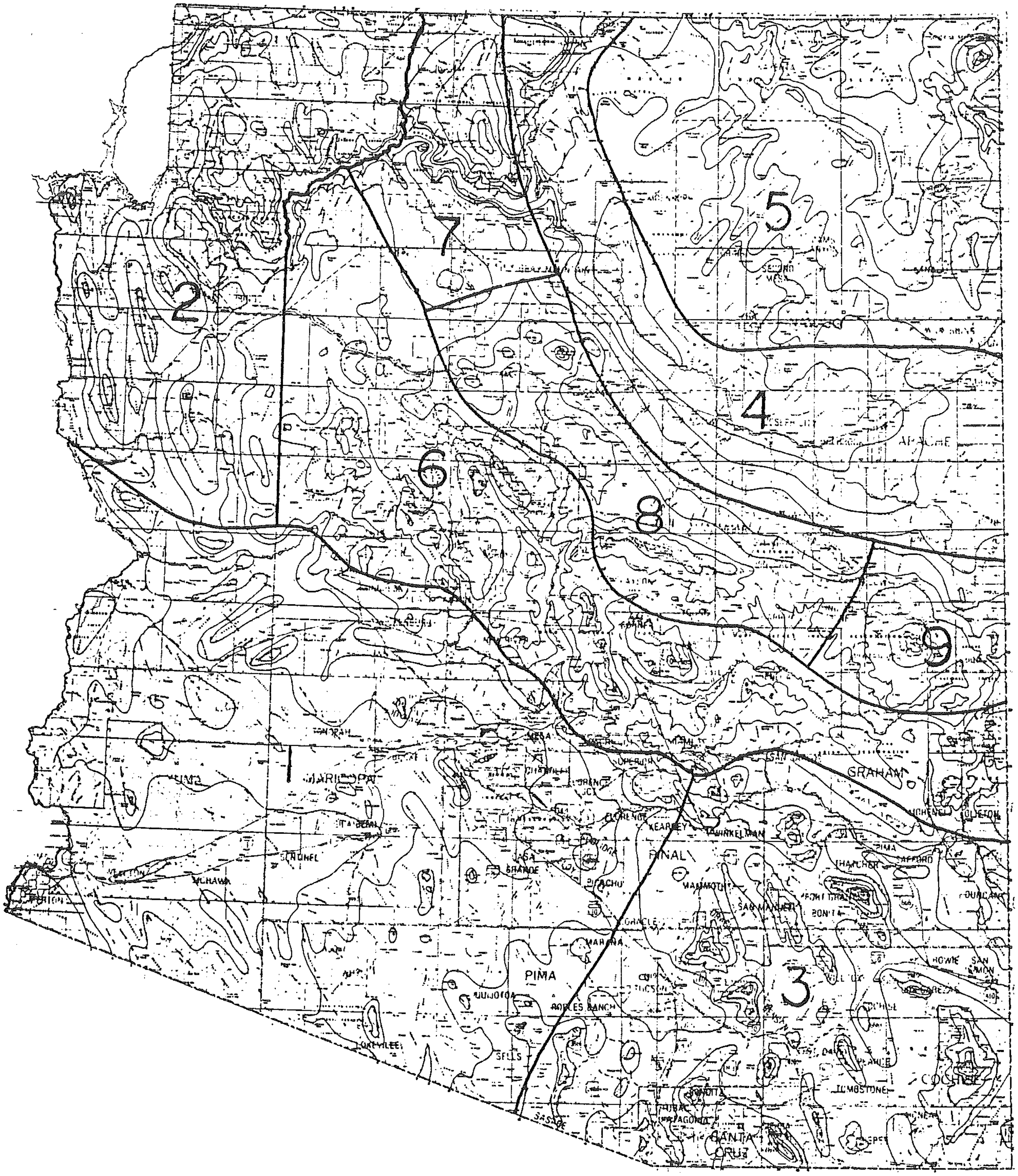

FIGURE 3-2. MAP OF CLIMATOLOGICAL ZONES IN ARIZONA

TABLE 3-1. LOCATION OF TEST SITES AND CLIMATIC ZONES

Site Number	Approximate Location	Route	Milepost	Climatic Zone
1	Benson	I10W	300.07	3
2	Gila Bend	I8E	112.80	1
3	Winslow	I40E	260.21	4
4	Minnelonka	I40E	261.78	4
5	Dead River	I40E	317.06	4
6	Flagstaff	I17N	337.0	8
7	Crazy Creek #1	I40E	322.72	4
8	Crazy Creek #2	I40E	323.78	4
9	Sunset Point	I17N	251.41	6
10	Seligman	I40W	131.71	6
11	Expo Hill	S87S	249.00	8
12	Benson East	I10W	303.00	3
13	Camron West	S64E	273.00	4
14	Jacob Lake	US89AN	578.00	7
15	Mohave	US93S	44.00	2
16	Tempe	US60E	191.00	1
17	Show Low	US60E	330.00	9
18	Morristown	US60W	120.00	1
19	McNary	US260E	369.00	9
20	Kingman	I-40E	59.00	2

Table 3-2. Cracking of the Selected Sites as Recorded in the ADOT Pavement Management System Data Base

	Year								
SITE	79	80	81	82	83	84	85	86	87
1	0	0	0	0	1	1	2	3	3
2	0	0	0	0	1	3	4	6	5
3	0	0	0	0	0	0	0	0	0
4	0	0	0	0	0	0	0	0	0
5	0	0	0	0	0	0	0	0	0
6	0	1	0	0	0	0	0	1	1
7	0	0	0	0	0	0	0	0	0
8	0	0	0	0	0	0	0	0	0
9	5	12	20	20	25	35	30	30	0
10	0	50	0	0	0	0	0	0	1
11	0	0	0	0	0	0	1	2	5
12	0	0	0	0	1	1	2	3	5
13	0	0	0	0	0	0	0	0	0
14	0	0	12	15	0	0	0	1	0
15	1	0	0	4	4	5	7	15	35
16	0	0	0	0	0	00	0	6	7
17	0	0	0	0	0	0	0	0	0
18	0	30	1	2	0	0	0	2	4
19	0	0	0	0	0	0	1	0	0
20	20	35	0	0	0	0	0	1	1

TABLE 3-3. ROUGHNESS OF THE SELECTED SITES AS RECORDED IN THE ADOT PAVEMENT MANAGEMENT SYSTEM DATA BASE

SITE	YEAR															
	72	73	74	75	76	77	78	79	80	81	82	83	84	85	86	87
1	39	43	36	52	55	48	39	28	72	79	47	77	83	110	103	110
2	33	49	53	65	66	38	80	59	96	100	73	86	80	109	96	90
3	41	64	71	103	161	185	168	97	49	81	82	97	99	139	114	143
4	30	56	62	102	144	157	192	103	54	96	91	82	95	118	134	131
5	180	211	35	39	57	116	84	89	92	117	97	132	78	90	100	114
6	61	92	54	91	112	132	142	149	182	64	72	74	67	109	126	101
7	228	269	324	49	62	112	82	93	107	179	153	210	200	219	233	220
8	198	234	263	28	45	99	57	54	77	101	75	112	85	127	110	137
9	27	47	75	72	105	96	108	132	142	174	166	187	201	209	210	90
10	36	62	53	77	124	127	180	198	256	99	77	96	91	126	134	226
11	208	203	231	211	200	230	0	0	172	190	166	197	168	177	197	167
12	121	0	48	67	80	77	88	113	129	149	173	152	139	170	169	204
13	219	253	278	315	320	333	359	197	208	242	235	232	238	218	226	221
14	160	187	106	129	147	148	176	126	138	134	143	172	177	171	205	180
15	79	109	107	151	163	102	122	121	120	133	138	140	157	138	175	171
16	65	70	47	64	71	86	131	0	96	110	94	94	101	103	89	80
17	0	280	166	143	161	185	175	161	49	69	64	91	94	134	106	95
18	29	51	63	72	78	130	103	99	98	134	97	128	138	133	119	120
19	109	215	128	139	191	244	259	93	109	141	139	89	101	119	117	123
20	35	37	44	46	59	34	70	81	103	53	55	63	59	104	112	91

TABLE 3-4. FRICTION NUMBERS OF THE SELECTED SECTIONS AS RECORDED IN THE ADOT PAVEMENT MANAGEMENT SYSTEM DATA BASE

SITE	YEAR					
	80	81	82	83	84	85
1	68	77	62	57	66	70
2	66	73	64	64	59	67
3	79	88	54	49	53	60
4	80	88	66	49	46	55
5	30	35	24	16	71	69
6	24	71	67	75	72	74
7	77	73	62	39	63	64
8	74	77	64	33	62	62
9	50	69	52	49	49	36
10	76	88	71	88	74	73
11	64		69		56	
12	78	77	52	50	60	70
13		81	64	71	72	64
14	83	67	43	47	78	
15	40	54	67	43	63	69
16		54	58	0	54	
17	73	75	69	66	67	
18	71	26	39	0	71	70
19	79	83	73	67	76	
20		77	76	77	74	

TABLE 3-5. INFORMATION OF TRAFFIC, MAINTENANCE, AND THE MOST RECENT CONSTRUCTION PROJECT AS RECORDED IN THE ADOT PAVEMENT MANAGEMENT SYSTEM DATA BASE

SITE	ADT	ADL	GROWTH FACTOR(%)	MAINT. COST($)	MOST RECENT PROJECT	YEA
1	15,592	2,830	2.2	298	I-10-5-46	76
2	5,462	1,220	0.7	70	I- 8-2-72	76
3	13,025	2,783	4.6	261	IRI-40-4-103	79
4	13,025	2,783	4.6	147	IRI-40-4-103	79
5	10,774	2,543	3.6	615	IR-40-5-66	84
6	16,246	1,846	5.4	5,551	I-17-2-85	81
7	10,738	2,535	3.6	22,227	I-40-5-44	75
8	10,738	2,535	3.6	1,438	I-40-5-44	75
9	17,575	1,616	4.3	225	I-17-1-65	69
10	8,115	1,382	3.7	6,283	I-40-2-86	81
11	7,295	354	4.3	0	DF-F053-1-9	77
12	14,095	2,544	1.1	1,100	IR-10-5-52	79
13	2,207	14	2.3	10	F033-1-505	79
14	1,342	61	3.0	7,060	F037-3-916	83
15	5,779	348	2.9	0	F039-1-908	77
16	23,898	265	0.3	226	F022-5-906	79
17	2,451	176	2.6	19	F026-1-513	79
18	7,956	290	1.9	0	BF022-2-940	83
19	1,487	65	0.0	1,963	F044-1-910	82
20	12,902	2,225	6.2	25	FRII-40-2-89	81

TABLE 3-6. HISTORICAL DATA FOR SITES

Site No.	ADOT designation	Date built	RC	AC	SC	RM	ACFC	BS	BTB	CTB	AB	SM	SGS
1	I-10 WB	1942						2.0			3.0	12.0	
	MP 300.07	6/1965		4.0			0.5						
		9/1975		1.3			0.5						
2	I-8 EB	5/1955		2.0							3.0	6.0	
	MP 112.8	1970		1.3			0.8						
		1972			0.3								
		1976					0.5						
3	I-40 EB	7/1958		3.5	0.3				3.0			6.0	
	MP 260.21	9/1971		1.3			0.5						
		6/1975			0.3								
		12/1979		6.0			0.5						
4	I-40 EB	7/1958		3.5	0.3				3.0			6.0	
	MP 261.78	9/1971		1.3			0.5						
		6/1975				0.3							
		1979		6.0			0.5						
5	I-40 EB	7/1960		4.0	0.3					6.0		6.0	
	MP 317.06	11/1973		2.8			0.5						
		1984		1.5			0.5						
6	I-17 NB	8/1960			0.3			1.0			6.0	10.0	12.0
	MP 337	9/1966		3.5	0.3								
		1970		5.5									
		1974					0.5						
		6/1981	5.5*	1.0									
7	I-40 EB	9/1961		4.0	0.3					6.0		6.0	
	MP 322.72	10/1975		2.5		0.3	0.5						
8	I-40 EB	9/1961		4.0	0.3					6.0		6.0	
	MP 323.78	10/1975		3.0		0.3	0.5						
9	I-17 NB	4/1967		3.5				2.0			2.0	17.0	6.0
	MP 251.41	1969					0.5						
10	I-40 WB	1969		3.5			0.8				6.0	22.0	
	MP 131	1981	4.0*	1.5			0.5						
11	SR-87 SB	1958						2.0					
	MP 249	1968			0.3								
		1976		2.5		0.3	0.5						

* No new thickness

TABLE 3-6. HISTORICAL DATA FOR SITES (CONT.)

Site No.	ADOT designation	Date built	RC	AC	SC	RM	ACFC	BS	BTB	CTB	AB	SM	SGS
12	I-10 WB	1967		3.5			0.5				6.0	15.0	
	MP 303	1979		2.0			0.5						
13	SR-64 EB	1936						2.5			3.0		
	MP 273	1979		3.0									
14	US-89A NB	1938						1.5					
	MP 578	1967			0.3								
		1974			0.3								
		1978		1.5									
		1979			0.3								
		1983			0.3								
15	US-93 SB	1936						2.5			6.0		
	MP 44	1961		3.0									
		1975			0.3								
		1977		3.0									
16	US-60 EB	10/43						2				9	
	MP 191	9/72					0.5						
		9/77		3			0.5						
		10/79					0.5						
17	US-60 EB	/38						2				6	
	MP 330	8/69			0.3								
		5/74			0.3								
		10/79		1.5			0.5						
18	US-60 WB	/65		3	0.3						4	15	
	MP 120	3/74			0.3								
		6/83					0.5						
19	US-260 EB	/54						2			3	6	
	MP 369	9/70			0.3								
		6/78		1.5									
		10/82					0.5						
20	I-40 EB	9/67		3.5			0.5				4	15	
	MP 59	7/81		2.3			0.5						

TABLE 3-7. ABBREVIATIONS USED FOR MATERIAL TYPES

Abbreviation	Type of layer
RC	Recycled Asphalt Concrete
AC	Plant Mixed Asphalt Concrete
SC	Seal Coat
RM	Rubberized Membrane Seal Coat
ACFC	Asphaltic Concrete Friction Course
BS	Bituminous Treated Surface
BTB	Bituminous Treated Base
CTB	Cement Treated Base
AB	Aggregate Base
SM	Select Material
SGS	Subgrade Seal

sites (sites 6 and 10) have been recycled with a new AC and/or ACFC has been added.

Two sites have a bituminous treated base. Three sites have a cement treated base, and eleven sites have an aggregate base. Four sites do not have a subbase layer. All other sites have select material for the subbase.

CHAPTER 4. FIELD WORK

Data were collected for each of the 20 sites. Three activities were performed at each of the sites; nondestructive testing, coring and sampling the pavement structure and cone penetration.

4.1. NONDESTRUCTIVE TESTING

One of the objectives of the project was to evaluate the ability of nondestructive tests, NDT, to generate the data required for overlay design. In the pavements field, nondestructive testing is synonymous with deflection measurements at the pavement surface. Originally ADOT used the Dynaflect for all NDT testing (Figure 4-1). The Dynaflect generates an oscillating load of 1000 lb transmitted to the pavement through rubber-lined steel wheels. Deflections are measured with five geophones, one between the load wheels and the other four are perpendicular to the load wheel axis spaced at one foot intervals as shown in Figure 4-2.

Due to the light load used to excite the pavement and the vibratory nature of the load, the Dynaflect has been criticized for not representing the stress condition generated by truck traffic. Falling weight deflectometers have been developed to overcome these shortcomings. ADOT purchased the first FWD imported to the United States by Dynatest. This unit was a prototype which generates the load impulse in the same manner as more recent FWD's but was operationally slow due to the need to manually place the deflection sensors and repeat loading the pavement for each sensor location. As a result, ADOT was in the process of upgrading its FWD at the start of the project to the current version manufactured by Dynatest. Since the new equipment was not available when the measurements were required, the services of ERES Consultants, Inc. of Champaign, Illinois were contracted to provide FWD data for sites 1 through 13 and site 15. The ERES Inc. FWD (Figure 4-3) is the same model as the FWD ordered by ADOT. In 1987, ADOT received its new Dynatest FWD which was later used to test sites 14 and 16 through 20.

The FWD is operationally simple. A mass is dropped onto a 11.8-inch plate with a rubber pad generating an impulse load on the pavement which is similar, but not identical to the stress pulse generated by moving trucks. The magnitude of the force on the pavement can be varied by altering either the mass of the drop weight or the drop height. The magnitude of the force generated on the pavement is directly measured with a load cell. Deflections are measured with seven geophones; one is placed at the center of the loaded area. The location of the other six sensors can be varied but are normally placed at one foot intervals as shown in Figure 4-4.

Based on the need to tie the historical deflection records with the new equipment purchased by ADOT, deflection measurements were performed with both the Dynaflect and the Dynatest FWD. The measurements with both instruments were made within a short time period to eliminate environmental factors from influencing the test results. The operational parameters of the Dynaflect are fixed. On the other hand, varying the drop mass and/or the drop height of the FWD provides a direct opportunity to evaluate the stress sensitivity of the materials in the pavement structure. Three force levels were selected to

FIGURE 4-1. DYNAFLECT

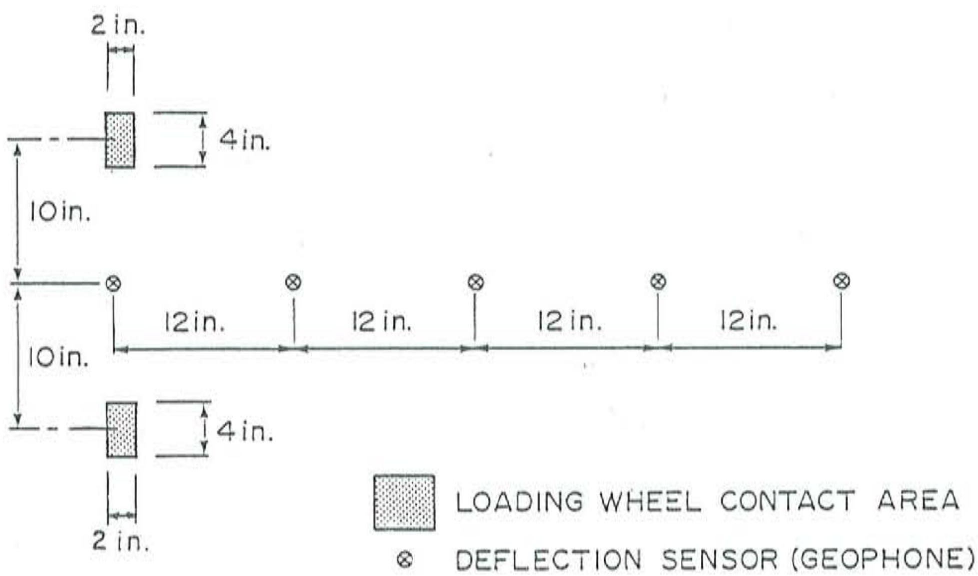

FIGURE 4-2. LOCATION OF LOADING WHEELS AND GEOPHONES OF THE DYNAFLECT

FIGURE 4-3. DYNATEST FWD

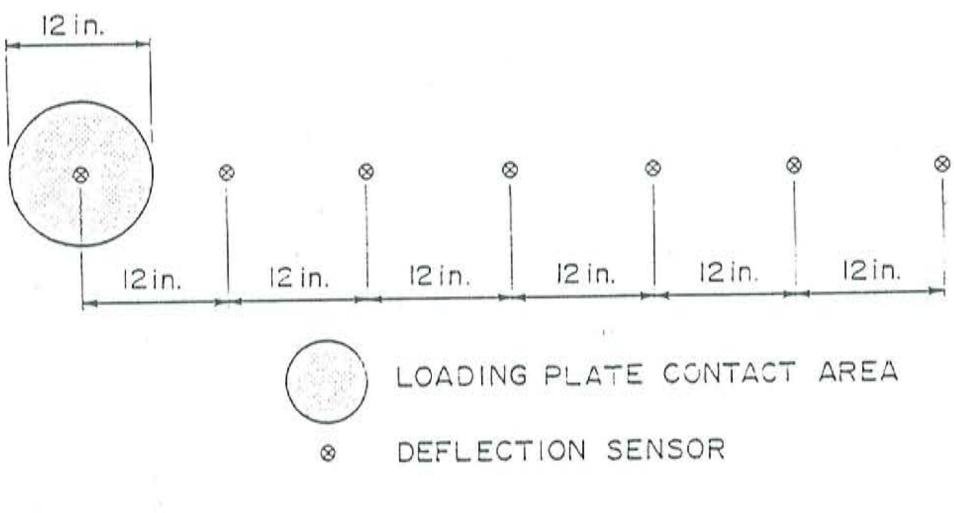

FIGURE 4-4. FWD: SENSOR LOCATIONS

simulate the load of an 18 kip axle, a lighter truck and a heavier truck. The target forces used in the field testing were 6, 9, and 12 kips by varying the drop height. The actual force generated on the pavement varies as a function of the stiffness of the pavement structure.

Deflection measurements were made in the outside wheel track of the pavement using the two devices. Ten stations, at 10 ft intervals within each site were measured on each test site. The pavement surface temperature was measured at the time of the test to allow for subsequent temperature corrections in the computed modulus values for the asphalt concrete layers. The FWD was operated at 3 stress levels (6, 9 and 12 kips) at stations 1, 5 and 10 at each site, while one stress level at 9 kips was used at the other stations. All 20 sites were tested with the FWD, while sites 1 through 13 and 15 were tested using the Dynaflect. A summary of the NDT data is shown in Appendix A.

4.2. SAMPLE COLLECTION

4.2.1. Description of Site Configuration

As mentioned earlier, at each site a total of 10 stations were established at a spacing of 10 ft apart. These stations were located in the right-hand wheel track of the right lane. Station 1 was set at a distance 1 foot ahead of the milepost marker corresponding to the site. Unless otherwise noted, the boring locations were at stations 1, 4 and 7.

4.2.2. Boring and Sample Equipment

Boring and sampling were accomplished through a subcontract with the firm of Foree and Vann. A CME-55 drill rig was used to accomplish sampling. Cores of asphalt concrete were obtained with a small portable electric powered coring device. Running water was used to cool the cutting bit of the 4" I.D. core barrel.

A 4 1/2" O.D. continuous flight auger was used to advance the hole after the asphalt concrete core had been removed. Undisturbed samples of subgrade materials were obtained by pushing 3" O.D., 2.8" I.D. thin-walled stainless steel sample tubes hydraulically with the drill rig.

4.2.3. Sampling Procedures

The procedure followed for this study may be summarized briefly as follows:

At stations 1, 4 and 7 of each site:

1) The asphalt concrete was cored, removed, and marked for identification.
2) The hole was advanced to the subgrade, using the cuttings to log the hole. Bag samples were obtained for index tests or tests on reconstituted samples.
3) A minimum of one thin-walled push tube sample of subgrade was obtained. In a few instances, the tube required driving with the 140 lb drop hammer.

4) The hole was backfilled and tamped in stages, and an asphalt cold patch plug approximately equal to the original thickness of the asphalt concrete was tamped into place.

More details on the sampling equipment are presented in Appendix B.

At some sites, it was noted that the layer thicknesses obtained from the boring logs did not exactly match the construction records provided by ADOT prior to sampling, especially site 14. Also, by visual observation of asphalt cores it was not possible in some cases to detect thin layers such as ACFC, SC, etc.

4.3 CONE PENETRATION TESTING

In order to more accurately determine the subsurface profile, and to detect layering, cone penetration testing (CPT) was performed at three locations at each test site. In general, these locations corresponded to station 1, the shoulder adjacent to station 1 (noted 1s) and station 4 (except where noted otherwise). The CPT consisted of advancing an electric friction cone penetrometer attached to a truck mounted CME 55 drill rig unit following ASTM procedure D3441-86 to depths of 25 feet or refusal. On occasion when refusal was met at relatively shallow depth, the cone penetrometer was removed, the hole was augered down to softer material and the cone was then re-advanced in the softer state.

Normal output of the CPT consists of a digital readout of the friction sleeve resistance in tsf and the cone tip resistance in tsf. These values are displayed every 4 in. and are average values over this 4 in. zone. Some typical plots of tip resistance vs. depth, are shown in Figures 4-5 and 4-6.

Although the CPT data consists of friction sleeve resistance along with the tip resistance, the only correlation for modulus which have been attempted are based entirely on soil type and the cone tip resistance (tsf). In addition, the friction sleeve values are somewhat temperature sensitive. Therefore, only the tip resistance was used in estimating modullus variation with depth.

The cone penetrometer data were used basically to determine the following:

1. Accurate subsurface profiling of each site, and
2. Possible correlation with modulus.

4.3.1 Determination of Subsurface Profiles

Friction ratio values were used to a limited extent, along with tip resistance values, the boring logs and the moisture content data in determining the subsurface profile at each site. This was to show the variation of soil type as well as stiffness, and therefore modulus, with depth and also laterally across a particular site. Figures 4-7 and 4-8 are examples of moisture content variations with depth.

4.3.2 Correlation between CPT Data and Modulus

In order to determine a possible correlation of cone tip resistance and modulus, it was first necessary to review the literature. Almost all correlations found in the literature contain a correlation of Young's modulus

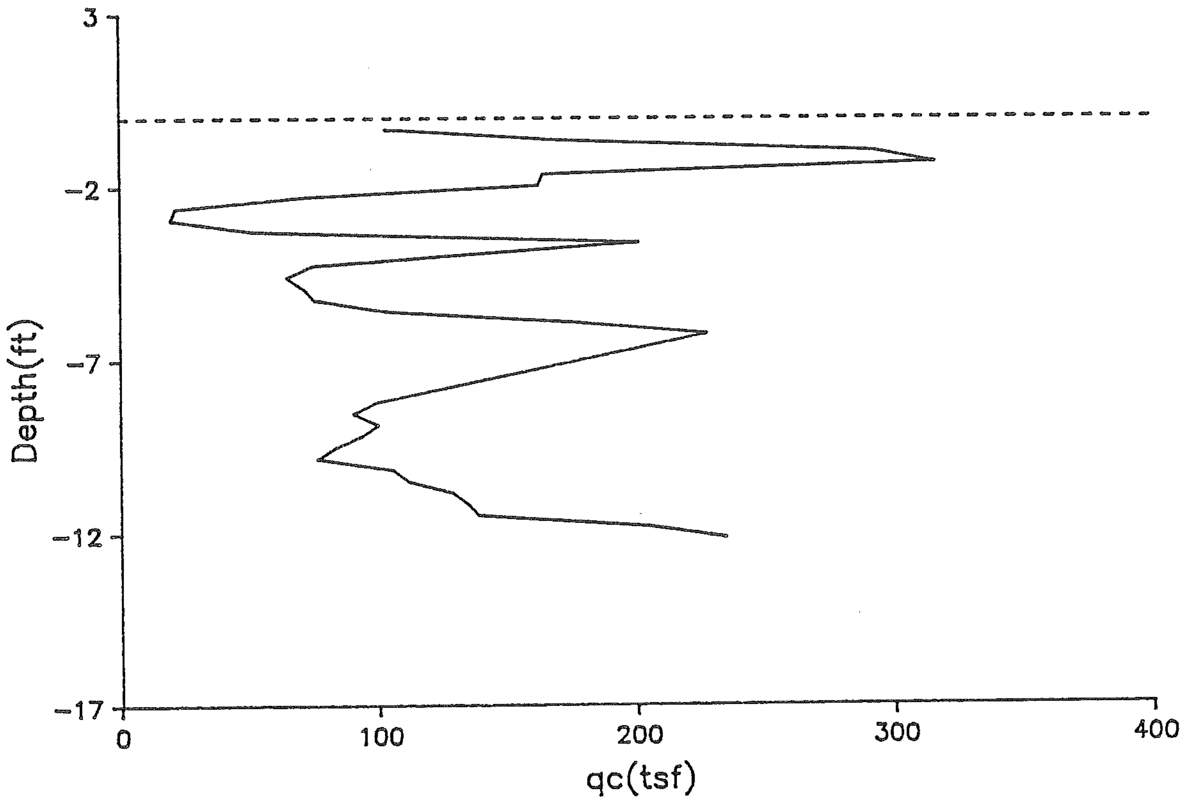

FIGURE 4-5. TYPICAL PLOT OF CONE RESISTANCE VS DEPTH (SITE 1, STATION 1, SHOULDER)

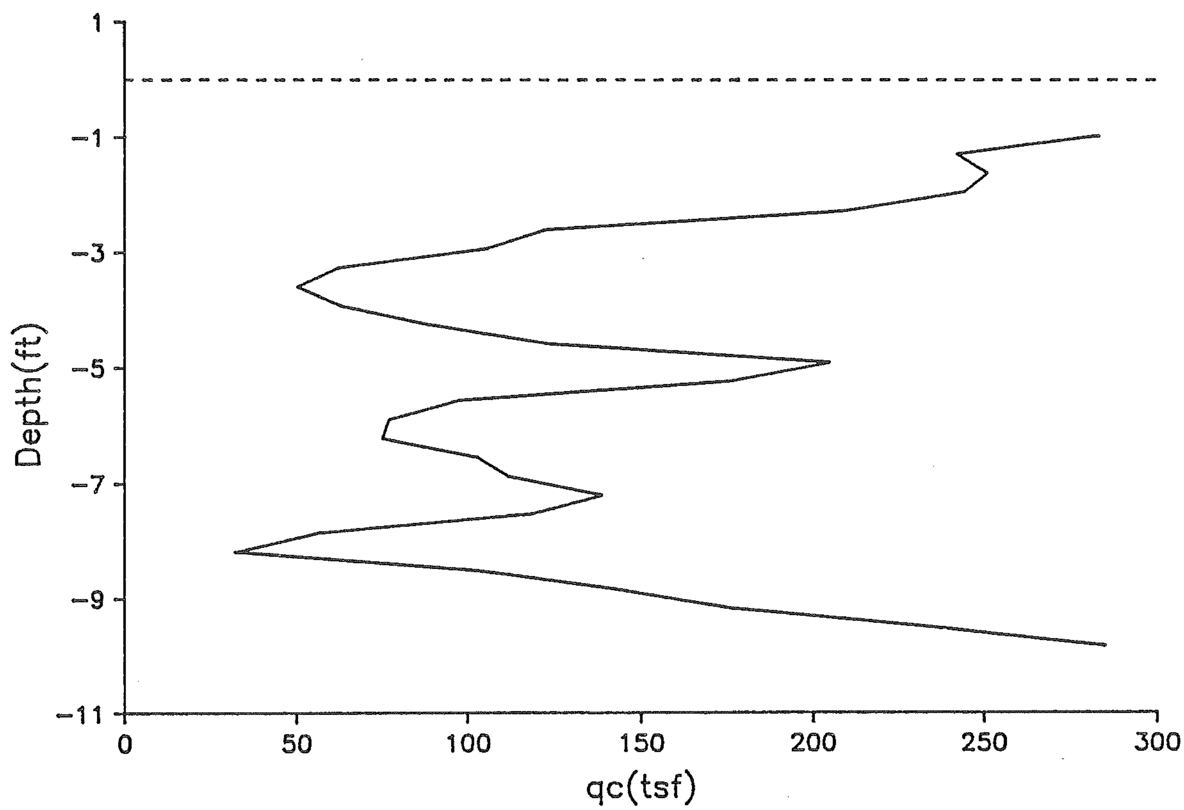

FIGURE 4-6. TYPICAL PLOT OF CONE RESISTANCE VS DEPTH (SITE 1, STATION 4)

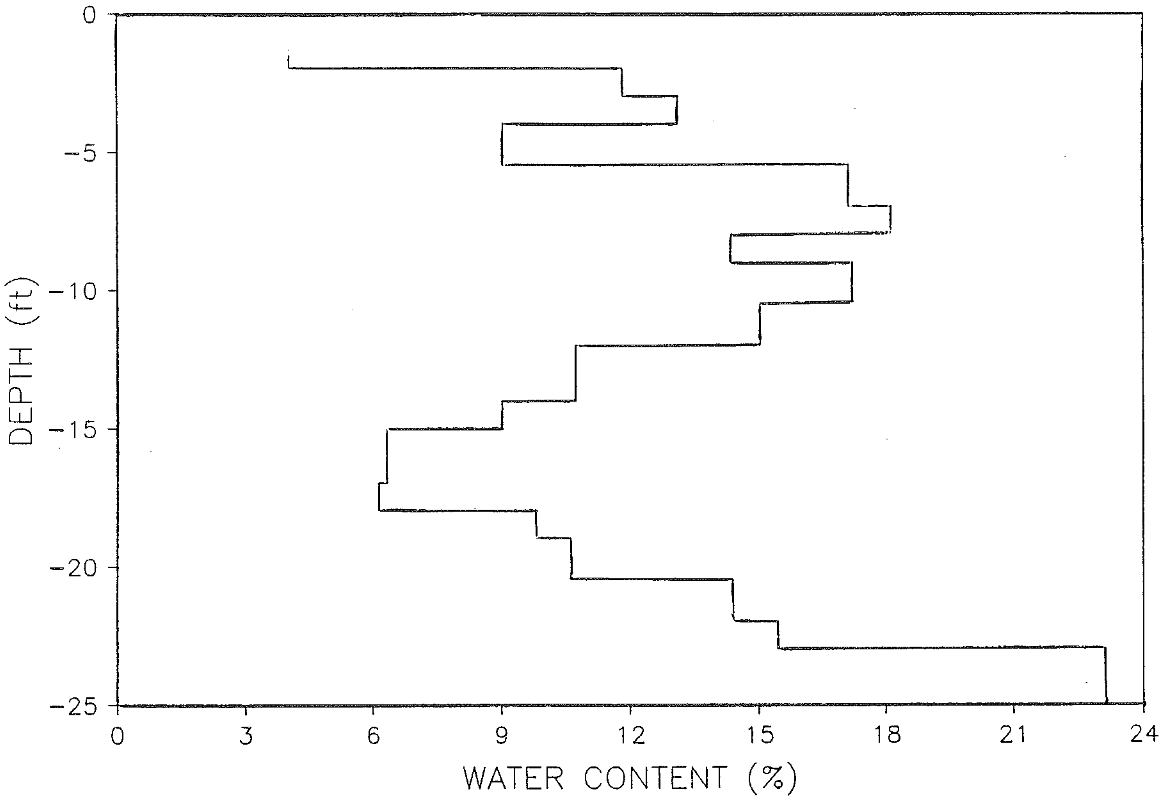

FIGURE 4-7 EXAMPLE OF MOISTURE CONTENT VARIATION WITH DEPTH (SITE 3, STATION 1)

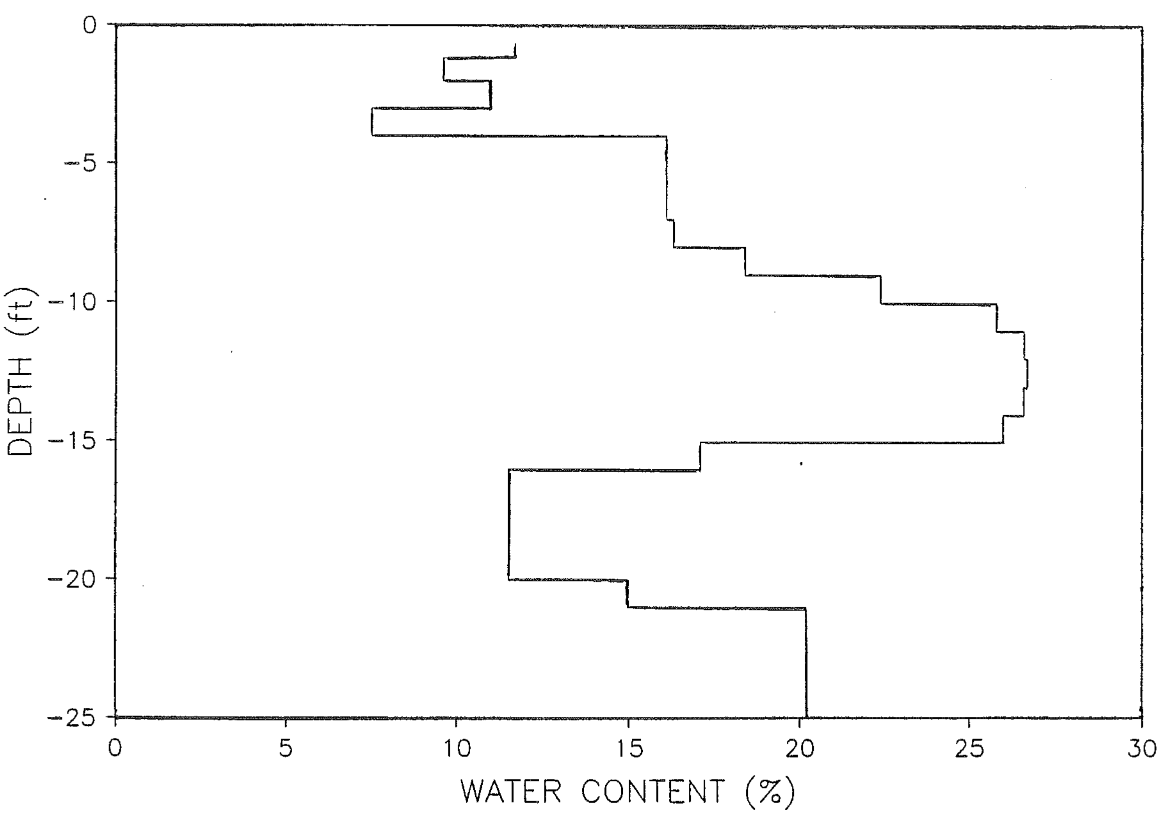

FIGURE 4-8 EXAMPLE OF MOISTURE CONTENT VARIATION WITH DEPTH (SITE 7, STATION 1)

and q_c of the form, $E = \alpha q_c$, with α values varying from 1 to 22. Values from the literature were used, together with our own laboratory data, to select α values. Heavier weight was attached to our laboratory values for this first trial analysis of the data. Accordingly, α were selected as follows:

CL: α = 50
CH: α = 30

Sands and Gravels: α = 10

These α values were then used to develop a layered profile of modulus vs. depth using the concept of a minimum modulus with all other values being multiples thereof. Figure 4-9 shows an example plot of E/E min. vs. depth where a remarkable variation of modulus vs. depth is exhibited. This plot, as well as Figures 4-5 and 4-6, which are typical, show that there is pronounced layering and that the q_c and the modulus are definitely not constant with depth. In fact, the modulus and q_c typically vary greatly with depth. It should be noted that previous studies have showed that the cone sleeve resistance is not correlated with the Young's modulus. Therefore, only the cone tip resistance was considered in this study.

Cone penetration resistance values measured in the traffic lane and on the shoulder were compared and it was found that the lateral variation was generally too great to suggest using test values from the shoulder location to represent values in the traffic lane.

Further analysis of the cone penetration data will be made as a part of a master thesis at ASU and a copy of this thesis will be transmitted to ADOT under separate cover.

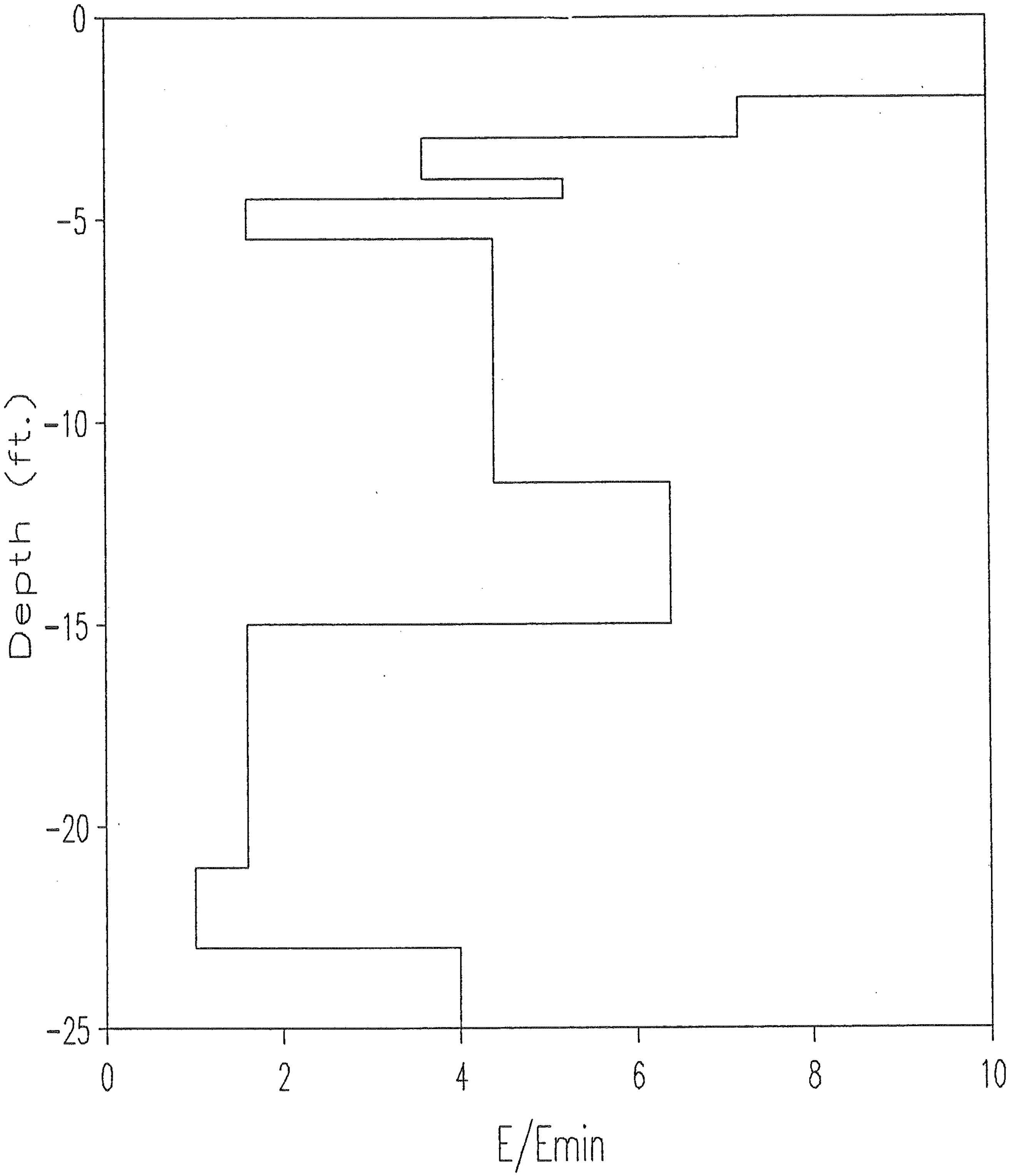

FIGURE 4-9 EXAMPLE PLOT OF E/E_{min} VS DEPTH

CHAPTER 5. LABORATORY TESTING

5.1. ASPHALT CONCRETE

5.1.1. Materials and Equipment

Asphalt concrete core samples of 4 in. diameter were collected from the 20 sites. By visual observation, it could be seen that some cores had only one distinct asphalt layer while some had two or three clearly defined asphalt layers. These distinct asphalt layers in the cores were most often separated by a seal coat or an asphalt concrete friction course. Samples were cut from these cores in such a way that a sample would be obtained from each distinct layer observed in the core. The thickness of the samples after trimming varied between 2 and 2.5 inches in most cases. However, several samples had a thickness of slightly less than 2 inches. A total of 34 asphalt concrete core samples were tested.

The resilient modulus equipment (Figure 5-1) was designed and fabricated at ASU to ASTM specifications D4123-82. It was similar to the equipment developed by Schmidt (57) with some modifications. It consisted mainly of a compressed air source, solenoid valve, timer, piston, loading frame, measuring devices and a two-channel chart recorder. The laboratory was equipped with a compressed air source which could be controlled by a pressure regulator and a surge tank. A solenoid valve activated by timer was used to provide pulses of compressed air. The compressed air was transmitted to a light pulsating load by means of the piston fixed on top of the loading frame. The load was applied across the vertical diameter of the specimen using two stainless steel loading strips with 0.5 in. width. The loading strips were curved at the interface with the specimen with a radius of 2 in.

The load was measured using a load cell attached to the top loading strip. The output voltage of the load cell was connected to one channel of the chart recorder and was precalibrated using static weights. The horizontal deformation of the specimen was measured using two Linear Variable Differential Transformers (LVDTs) connected to a special frame attached to the specimen. The output voltages of the two LVDT's were merged into one signal and connected to the other channel of the chart recorder. The outputs of the LVDTs were calibrated using a micrometer at temperatures of 41, 77 and 104°F which were used in the test.

The test was conducted inside a large controlled temperature room. A thermometer was buried inside a dummy specimen to indicate the actual temperature of the specimens. It took between 3-4 hours to change the temperature to the required test temperature.

5.1.2. Test Procedure

Before running the resilient modulus test, the saturated surface-dry bulk density of the specimens was determined according to ASTM D2726 procedure. The diametral resilient modulus test was then performed according to ASTM D4123-82 procedure. The following is a brief description of the testing procedure of the resilient modulus test.

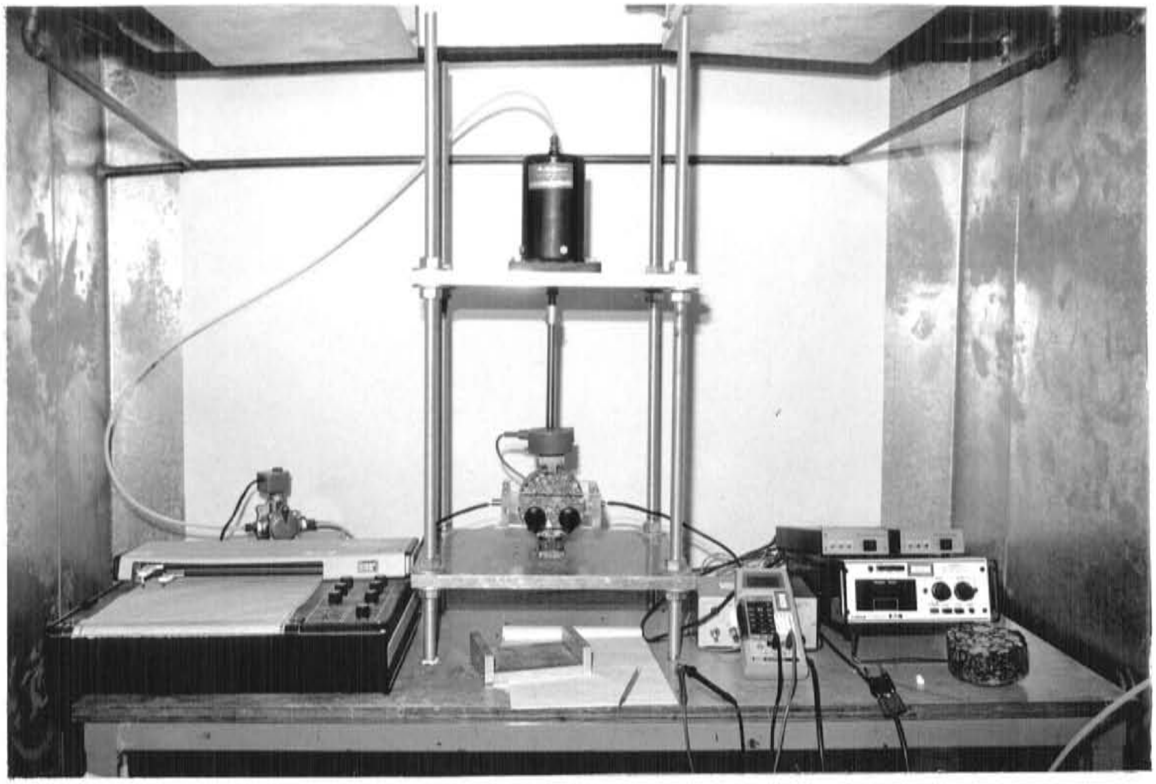

FIGURE 5-1. RESILIENT MODULUS MACHINE FOR ASPHALT CONCRETE TESTING

When the specimen reached the required test temperature it was placed in the resilient modulus test machine. Care was taken to ensure that the specimen was exactly centered between the two loading strips. The frame was then attached to the specimen and the LVDT's were glued to the specimen at its horizontal diametral plane. The output voltages of the LVDT's were adjusted in order that the LVDTs be used within their linear ranges. A pulse load of 30 to 85 lb was then applied across the vertical diameter of the specimen every 2 seconds with a duration of 0.1 second. The load was applied 150 times for conditioning the specimen before the results were recorded. The specimen was rotated 90° and tested again in the new position using the same steps. In order to reduce the permanent deformation in the specimen, testing was sequenced from 41°F then 77 and 104°F.

5.1.3. Test Results

A typical plot of load and horizontal deformation is shown in Figure 5-2. The instantaneous and total resilient moduli were calculated using the following equations.

$$E_{ri} = P(\nu_{ri} + 0.27)/t \cdot \Delta H_i \qquad (5\text{-}1)$$

$$E_{rt} = P(\nu_{rt} + 0.27)/t \cdot \Delta H_t \qquad (5\text{-}2)$$

where:

E_{ri} = Instantaneous resilient modulus of elasticity (psi)
E_{rt} = Total resilient modulus of elasticity (psi)
ν_{ri} = Instantaneous resilient Poisson's ratio
ν_{rt} = Total resilient Poisson's ratio
P = Repeated load (lb)
t = Thickness of specimen (in.)
ΔH_i = Instantaneous recoverable horizontal deformation (in)
ΔH_t = Total recoverable horizontal deformation (in)

Both instantaneous and total Poisson's ratios were assumed to be 0.3, 0.35 and 0.4 at temperatures of 41, 77 and 104°F, respectively. The modulus is taken as the average of the two values obtained in the two perpendicular positions. Tables 5-1, 5-2 and 5-3 show a summary of the density, instantaneous resilient modulus and total resilient modulus of the specimens at test temperatures of 41, 77 and 104°F, respectively. Detailed resilient modulus data are presented in Appendix C.

The resilient modulus results show that the modulus value decreases when the temperature increases. Also, the instantaneous resilient modulus is typically larger than the total resilient modulus and they are well correlated. The use of the instantaneous resilient modulus is more common than the total resilient modulus since the former represents the "elastic" modulus of the material more than the latter. The instantaneous modulus was used in Chapter 6 for comparison with the back-calculated moduli obtained from the NDT data.

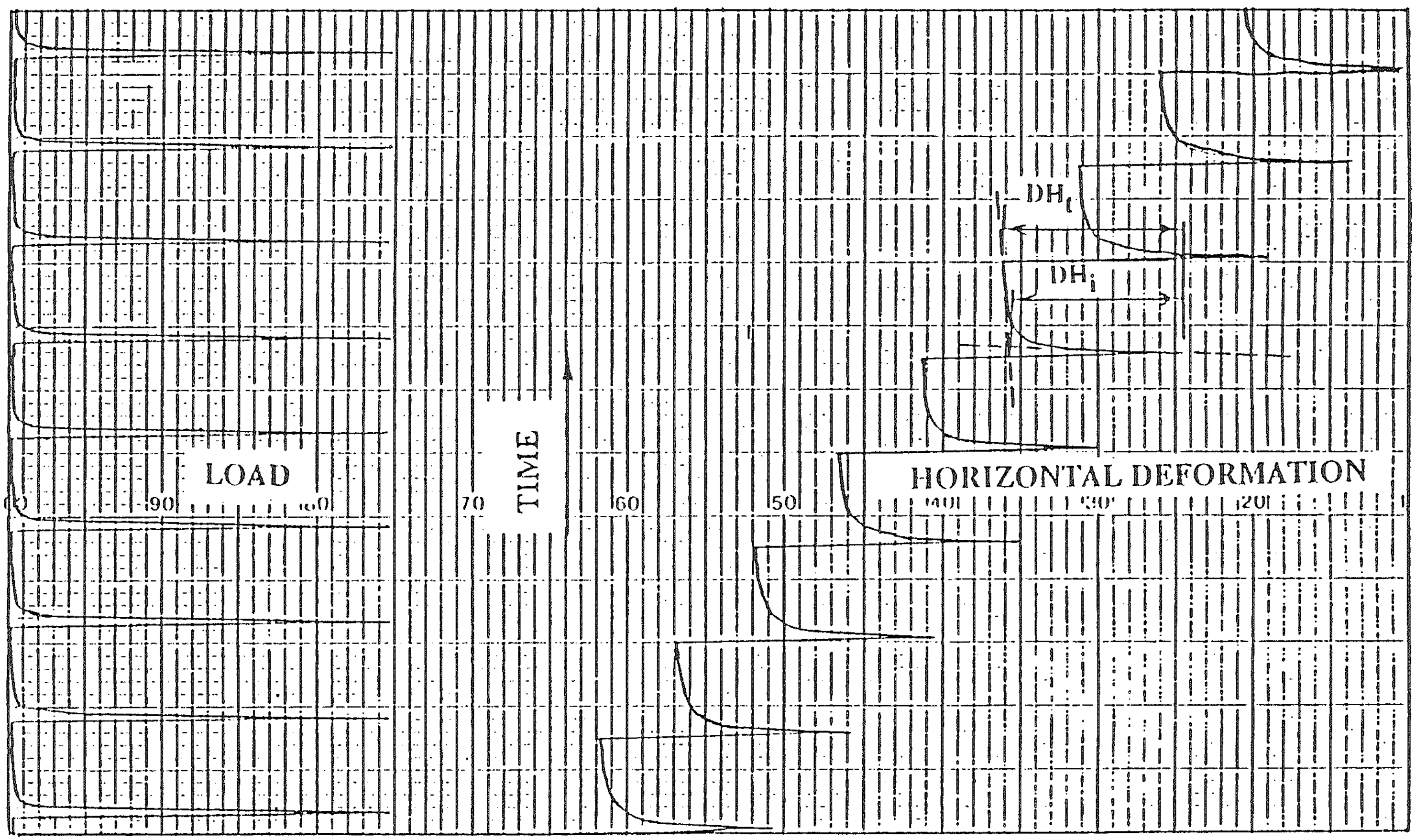

FIGURE 5-2. TYPICAL LOAD AND HORIZONTAL DEFORMATION OBTAINED DURING THE RESILIENT MODULUS TEST

Table 5-1. Summary of density and average resilient moduli of asphalt concrete samples at 41 F

Site/ Station/ Sample no.	Density (pcf)	Average inst. resilient modulus (ksi)	Average total resilient modulus (ksi)
1/1/1	129.4	1226	1062
2/1/1	148.7	3045	2131
2/1/2	146.8	3111	2705
3/1/1	135.2	3292	2532
3/1/2	145.7	1067	910
3/7/1	134.7	5377	4067
4/1/1	132.1	3638	2430
4/1/2	146.6	4016	1906
5/4/1	167.5	2446	1936
5/4/2	145.4	1397	1194
6/1/1	146.5	2133	1400
6/1/2	135.2	1875	804
6/1/3	141.9	1376	977
7/4/2	153.8	2334	1794
8/1/1	150.7	1075	821
8/1/2	141.6	1507	1162
9/1/1	144.0	1858	1186
9/1/2	147.7	3567	2945
10/4/2	153.1	2855	2217
11/5/1	154.0	3776	2937
12/1/1	146.8	2268	1564
12/1/2	146.2	4939	2573
13/1/1	156.9	3778	3181
13/4/1	158.2	2470	2117
14/4/1	140.2	1155	920
15/4/1	146.7	2879	1869
15/4/2	152.4	2924	2215
16/1/1	148.9	2993	2589
17/1/1	142.3	1427	1148
18/1/1	147.9	2586	2277
19/4/1	125.6	1315	1176
19/4/2	124.3	950	842
20/1/1	148.3	3182	2786
20/1/2	145.7	4850	4021

Table 5-2. Summary of density and averagee moduli of asphalt concrete samples at 77 F

Site/ Station/ Sample no.	Density (pcf)	Average inst. resilient modulus (ksi)	Average total resilient modulus (ksi)
1/1/1	129.4	1209	1036
2/1/1	148.7	999	829
2/1/2	146.8	541	378
3/1/1	135.2	814	642
3/1/2	145.7	675	618
3/7/1	134.7	1376	1173
4/1/1	132.1	1319	1097
4/1/2	146.6	1269	1088
5/4/1	167.5	987	681
5/4/2	145.4	411	310
6/1/1	146.5	549	403
6/1/2	135.2	892	709
6/1/3	141.9	487	340
7/4/2	153.8	1672	1430
8/1/1	150.7	700	539
8/1/2	141.6	426	374
9/1/1	144.0	761	599
9/1/2	147.7	1557	1230
10/4/2	153.1	1312	992
11/5/1	154.0	2191	1920
12/1/1	146.8	641	503
12/1/2	146.2	1593	1356
13/1/1	156.9	954	693
13/4/1	158.2	1049	829
14/4/1	140.2	518	409
15/4/1	146.7	657	473
15/4/2	152.4	1135	860
16/1/1	148.9	1569	1422
17/1/1	142.3	630	532
18/1/1	147.9	1219	1031
19/4/1	125.6	741	623
19/4/2	124.3	645	551
20/1/1	148.3	1093	863
20/1/2	145.7	2242	1727

Table 5-3. Summary of density and average resilient moduli of asphalt concrete samples at 104 F

Site/ Station/ Sample no.	Density (pcf)	Average inst. resilient modulus (ksi)	Average total resilient modulus (ksi)
1/1/1	129.4	133	110
2/1/1	148.7	76	66
2/1/2	146.8	--	--
3/1/1	135.2	398	359
3/1/2	145.7	329	289
3/7/1	134.7	--	--
4/1/1	132.1	822	696
4/1/2	146.6	757	645
5/4/1	167.5	76	68
5/4/2	145.4	137	119
6/1/1	146.5	77	66
6/1/2	135.2	412	347
6/1/3	141.9	--	--
7/4/2	153.8	787	661
8/1/1	150.7	156	141
8/1/2	141.6	168	131
9/1/1	144.0	88	66
9/1/2	147.7	460	372
10/4/2	153.1	254	205
11/5/1	154.0	505	423
12/1/1	146.8	272	226
12/1/2	146.2	960	886
13/1/1	156.9	127	107
13/4/1	158.2	528	457
14/4/1	140.2	128	102
15/4/1	146.7	331	259
15/4/2	152.4	472	403
16/1/1	148.9	665	522
17/1/1	142.3	286	231
18/1/1	147.9	230	201
19/4/1	125.6	171	146
19/4/2	124.3	117	99
20/1/1	148.3	109	84
20/1/2	145.7	976	841

5.2. BASE AND SUBBASE MATERIALS

Samples of base and subbase materials were collected from the 20 sites. The base course material is either bituminous treated, cement treated or unstabilized aggregate as shown in Table 3-6. The subbase material is select material.

Sieve analysis tests were performed on samples of untreated aggregate and select materials at the first 15 sites. The gradation of these materials are shown in Table 5-4.

Bituminous treated bases could not be tested for resilient modulus because the samples did not have smooth surfaces. One CTB sample obtained from site 7 was tested for resilient modulus and the corresponding modulus was 500 ksi. The test proved that the diametral resilient modulus machine can be used for testing CTB samples; however, a large load has to be applied (about 80 lb) in order to get a measurable deformation.

5.3. SUBGRADE MATERIALS

5.3.1. Equipment

An automated microcomputer-controlled triaxial testing system was used to measure the resilient modulus of the subgrade materials in the laboratory. A copy of a photo of the apparatus is shown in Figure 5-3. The system can be described in major components as follows.

(1) Load Frame and Test Chamber

The base of the load frame is a thick anodized aluminum plate which is attached to the upper cross-head beam with 1 1/2" stainless steel threaded rods with nuts. The test chamber is comprised of anodized aluminum bottom and top plates, held together with large ss hex rods. Compressed between the top and bottom cell plates is a 5" I.D., 1/4" wall plexiglass tube, to provide visibility of the specimen. The test chamber is equipped with a very low friction "air bushing" and the piston is guided with two ss Thompson ball bushings. The axial load on the piston was measured with an interface load cell and the vertical displacements were measured with two schaevitz LVDT's. Other transducers available, but not used in this test series, include validyne differential pressure transducers for effective stress, cell pressure, and volume change. However, a regulated back pressure was applied through the specimen base and held constant as an internal pore air pressure and a regulated external air pressure was held constant inside the cell. The difference between these pressures was reported as the confining stress. The axial load on the piston was generated with a 2" I.D. double-acting air piston loader with a 3" stroke. A constant, regulated pressure, called the "steady" pressure, was applied to the lower chamber of the double-acting piston. The pressure applied to the upper chamber was termed the "cyclic" pressure because it was caused to "cycle" by the cyclic loading control unit. The deviator load on the test specimen (which was 2.8" in diameter and

TABLE 5-4. GRADATION OF AGGREGATE AND SELECT MATERIALS AT VARIOUS SITES

Site	1	2	3	4	5	6	7	8
Sampling Depth (in.)	12-24	8-17	15-20	13-16	13-19	9-19	14-20	18-23
Material Type	Select	Select	Select	Select	Select	Aggregate/ Select	Select	Select
% Passing								
No. 4	88	76	97	95	96	65	93	99
No. 8	64	62	91	91	92	40	88	96
No. 16	45	49	82	83	90	27	81	92
No. 30	30	38	60	66	86	20	69	83
No. 50	16	26	23	33	72	13	42	51
No. 100	4	14	5	11	39	8	14	14
No. 200	0	4	2	4	22	4	5	4

TABLE 5-4. GRADATION OF AGGREGATE AND SELECT MATERIALS AT VARIOUS SITES (CONTINUED)

Site	9	10	11	12	12	13	14	15
Sampling Depth(in.)	10-36	12-25	-----	6-12	12-30	7-11	9-13	9-14
Material Type	Select	Select	None	Aggregate	Select	Aggregate	Aggregate	Aggregate
% Passing								
No. 4	78	89		63	99	58	46	82
No. 8	63	78		44	95	43	35	66
No. 16	50	68		31	86	29	25	50
No. 30	38	56		19	72	18	17	33
No. 50	25	41		9	57	11	12	15
No. 100	14	24		4	36	7	8	6
No. 200	7	12		2	12	4	4	2

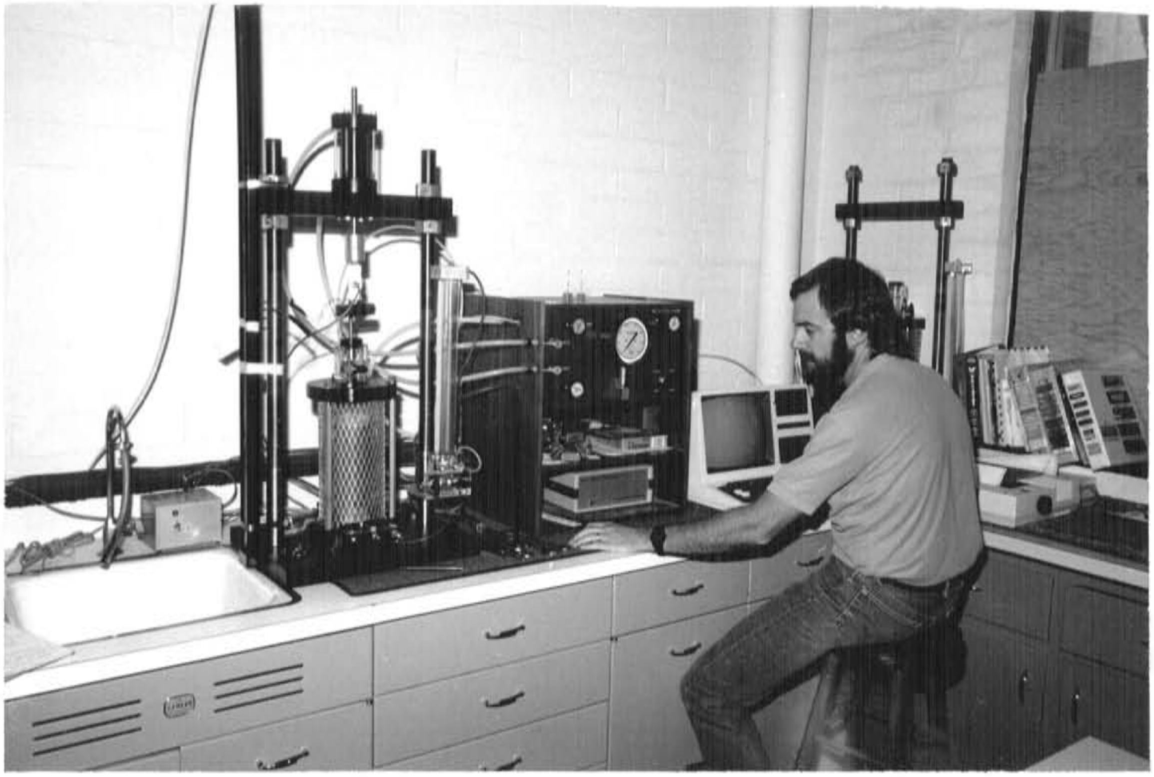

FIGURE 5-3. TRIAXIAL RESILIENT MODULUS APPARATUS FOR SUBGRADE MATERIAL TESTING

about 6.5" to 7" high) corresponded to the amount by which the cyclic pressure exceeded the steady pressure.

(2) Signal conditioning unit

The analog signals from the load cell, LVDT's, and cell pressure transducer were transmitted to a 20-channel Validyne module case, which houses the signal conditioning module for each channel of data. Signal conditioning includes amplification as required so that all signals ranged from 0 to about 10 VDC full scale. Each signal could be displayed one at a time on the digital voltmeter in the Validyne, for checking or calibration. Other signal conditioning included the use of a non-inverting summing amplifier to average the signals from the two LVDT's before transmission to the Validyne.

(3) Process Interface

After amplification to the 0-10 VDC range the signals were transmitted in analog from a Process Interface, a unit manufactured by S and L Instrumentation Co. This unit serves as an interface between the Validyne and the microcomputer. The signals are further conditioned in the process interface, including conversion from analog to digital form, before transmission to the microcomputer.

(4) Microcomputer

A TRS-80 Model 4 microcomputer is used via a series of software packages to collect, reduce, and plot the data. During the test itself, the software package provides closed-loop control of the test. The programs are mostly interactive so the user can specify the desired test conditions, such as stress control vs. strain control, desired rate of load increase, pulse shape for dynamic loading, confining stress, drainage conditions, etc. Test control is accomplished as follows.

a) Readings from each channel are collected and reduced by the computer.
b) A comparison is made between the results obtained and the test conditions desired (e.g., for strain rate control, the strain rate obtained is compared with the strain rate requested)
c) The computer sends a command (in digital form) to the Process Interface, as needed to correct the test condition.
d) The Process Interface converts the digital command to a voltage and sends the voltage to the electro-pneumatic transducer inside the cyclic loading control unit.
e) The e/p transducer converts the electrical signal to a pulse of air pressure with the same shape as the electrical signal.
f) The pulse of air pressure is amplified (boosted) and then transmitted to the "cyclic" chamber of the double-acting loading piston.
g) The response to this new increment in load is then registered by the transducers and transmitted to the computer, thus "closing the loop." Cell pressure is likewise computer controlled as required.

The microcomputer is also connected to dot-matrix printer which displays data in tabular and/or graphical form.

(5) Cyclic Loading Control Unit

The control unit is a cabinet which houses a variety of components including air filter, e/p transducers, volume boosters, relays, switching valves, pressure gages, and pressure regulators. Some of these components are used to control test conditions manually, such as steady and back pressures, while other components are under computer control.

5.3.2. Calibration

The LVDT's were calibrated individually with the use of a micrometer to determine their personal calibration factor and linear range corresponding to this factor. They were then attached to the triaxial apparatus and wired into the non-inverting summing amplifier to determine the calibration factor of both LVDT's together. This was performed with the aid of an axial dial gage which was also attached to the triaxial cell. The piston was then moved a known distance on the dial gage and the corresponding voltage was recorded from the Validyne signal conditioning unit.

The load cell (Interface - SSM 1000) was calibrated with the aid of a proving ring which had previously been calibrated with Bureau of Standards traceable weights. The static calibration was performed by varying the pressure on the loading system and noting the corresponding proving ring deflection and voltage.

Due to the dynamic loads and the duration of load (0.2 sec), a dynamic calibration of the load cell and the LVDT's was performed using an oscilloscope. The peaks were recorded on the oscilloscope and were then compared to the computer output. This was performed at various different loads and deflections to get an average correction factor. This factor was determined to be 1.042 for the load cell and 1.11 for the LVDT's. The overall correction factor, the load cell factor divided by the LVDT factor, was 0.9387, and this factor was multiplied directly to the calculated modulus values to obtain resilient modulus values corrected for dynamic response.

5.3.3. Testing Procedure

The testing procedure followed in measuring the resilient moduli of the subgrade materials was based generally on the AASHTO-T274-82 procedure. However, it was deemed necessary and desirable to deviate from the AASHTO procedure in a number of aspects which will be discussed in this section. Before discussing these deviations, however, it is necessary to review the definition of the resilient modulus and to make clear what is meant by stress level and stress level sensitivity.

(1) Resilient Modulus

The resilient modulus is defined as the ratio of the repeated stress to the recoverable strain. Therefore, the intent of the pre-conditioning loading phase of the resilient modulus test is to induce any plastic strains which are prone to occur, so that mostly elastic strains remain when loading to measure resilient modulus occurs later. Ideally, the pre-conditioning loading phase would entail application of stresses comparable to those imposed by traffic loads when the test specimen was in-situ. If the sampling and specimen preparation process were "perfect," i.e., disturbance-free, then reapplication of traffic loads would produce no new plastic strains because plastic strains would have already occurred in-situ. However, the sampling process is not "perfect" and some plastic strains do occur during pre-conditioning. Pre-conditioning is an attempt to erase the effects of disturbance. The degree to which this attempt is generally successful is difficult to assess, but there is no doubt that pre-conditioning loading tends to erase the effects of disturbance.

(2) Stress Level

It is a well-established fact that when stresses on a soil specimen are increased to a level higher than ever applied previously, plastic strains will occur. Therefore, resilient modulus cannot be measured for such a cycle of loading. Stresses may be described broadly as either normal stresses or shear stresses. When discussing stress level it is important to distinguish between normal stress level and shear stress level, because normal and shear stresses produce somewhat differing effects on a soil specimen. When a specimen is "over-stressed" by normal stress, plastic strains occur and bonds between particles are broken. However, they are reformed at higher normal stress and the net effect of having been loaded to a higher normal stress is that the specimen is now denser, stiffer, and stronger than it was. By contrast, when the shear stress is raised to a level higher than ever before, plastic strains result in the breaking of bonds which either do not reform or new bonds which are typically weaker than previous bonds. Therefore, the net effect of increasing the shear stress to a new high is to produce a specimen which is softer and weaker than before. Thus, the effect on modulus of shear stress elevation is opposite to the effect of normal stress elevation. In the laboratory, separation of and distinction between shear and normal stresses is relatively easy. In the field, wheel loads produce both shear and normal stresses, and which effect is likely to predominate varies with the point of consideration within the pavement structure.

(3) Stress Level Sensitivity

In light of the preceding discussion, it is obvious that the measured modulus would be "sensitive" to an increase in either normal or shear stress to levels higher than ever applied before. However, in this case, plastic strains would occur and resilient modulus could not be measured. Thus resilient modulus stress level sensitivity must be quantified only when the following conditions are met:

a) The stresses applied (both shear and normal) are less than or equal to the maximum level of stress previously applied.
b) The stress has been applied a sufficient number of times that the strains become essentially entirely recoverable (elastic).

This means that quantification of resilient modulus sensitivity to stress level for this research project corresponds to assessing the extent to which the elastic strains exhibit non-linearity.

With the proceeding background discussion and definitions established, it is now possible to efficiently describe the deviations from the AASHTO Resilient Modulus test procedure.

(4) Deviations from the AASHTO-T274-82 Procedure

After a careful examination of the AASHTO Procedure it was concluded that the following deviations were justified.

a) Stress State. As part of pre-conditioning the AASHTO Procedure calls for levels of both normal and shear stresses which are in most cases well beyond those estimated to have been applied by in-situ traffic loading. For example, T274 calls for application of shear stresses to triaxial specimens of clayey soils when the confining pressure is zero, a condition which never exists for a subgrade in-situ. Accordingly, a pre-conditioning program for each site was established as follows.

   1. The pavement structure geometry was established for each site from the boring logs.
   2. Moduli for the various layers were estimated from available back-calculated values based on NDT data.
   3. Maximum past stress state was estimated using the computer program ELSYM5, together with an assumed axle overload to 22 kips. For this computation the modulus of the asphalt concrete was adjusted in accordance with available pavement temperature data.
   4. The computed stresses were expressed in terms of octahedral shear and normal stresses and formed a "triangle" representing the maximum past stress states for the subgrade at each site. An example of a stress triangle is shown in Appendix E.
   5. A conditioning program and a testing procedure were then established for each test specimen using the load triangle. In general, each specimen was conditioned for 1000 cycles at a low state of stress, 1000 cycles at a medium state of stress, and 2000 cycles at the maximum state of stress, corresponding to the apex of the triangle. The specimen was then loaded for 200 cycles at various lower stress states, to measure the resilient modulus and to check for stress level sensitivity.

b) Pre-conditioning. The AASHTO Procedure calls for pre-conditioning by cyclic loading to only 200 cycles at each stress state. It was consistently found that cyclic loading to several thousand cycles was needed to remove the plastic strains.

c) Preparation of Specimen Ends. In order to assure an intimate contact between the specimen ends and the end platens, a layer of Burkestone -- a quick hardening cement -- was placed on the platens and allowed to set-up with the platens in place and the loading piston aligned and screwed into the top cap. If a bonding agent like this were not used, the interfaces between the specimen and the end platens might be compressible and produce significant error in the measured modulus.

An outline of the sample preparation and the Triaxial Test Sequence used is given in the following sections.

(5) Sample Preparation

The following procedure was used in preparing a sample for resilient modulus testing:

a) Cut sample tube to size (if necessary) with a hacksaw. Clean inside of tube with a deburrer to ensure smooth surface for extrusion.
b) Trim sample bottom until flush and smooth.
c) Place Burkestone (high strength, fast setting cement) on greased cap and place on trimmed sample bottom.
d) Let cement harden and remove cap.
e) Mark location of porous stone in the Burkestone and drill a small hole for air communication.
f) Mark tube and base to assure hole alignment.
g) Place thin layer of Burkestone on base (around porous stone), line up marks and place on sample bottom.
h) Place tube in extruding apparatus and apply a small pressure to allow a good bond between two layers of Burkestone. Let set for 15 minutes, or until hard.
i) Extrude until 7 inches of sample is still in tube.
j) Trim off excess soil, dig soil down 5mm maximum and make level.

(6) Triaxial Test Sequence

After the specimen has been extruded, weighed, and measured, the following steps are followed to prepare the sample for testing.

a) Screw the specimen base into the bottom of the triaxial cell.
b) Screw the loading piston into the specimen cap, place a thin layer of Burkestone on the cap, loosen ram screw, and place entire top of triaxial cell on top of the three tie rods and confirm centering. Ease piston down by hand until Burkestone is in contact with sample top. Vibrate the piston until the entire surface of the specimen top is covered with Burkestone and there are no voids between the cap and the specimen. Let Burkestone set until hard, usually about 15 minutes.
c) Holding cap by hand, screw out piston and remove entire top assembly. Place membrane in membrane expander and apply a vacuum to the expander to pull membrane out tight. Place membrane over specimen, remove vacuum and pull membrane away from expander.
d) Place o-rings on o-ring expander and place one on the base and then one on the cap over the membrane.
e) Assemble entire cell including plastic chamber, screw piston into cap, tighten down top of cell and then tighten piston ram screw.
f) Place in the loading frame, align and attach piston to clamp, then clamp triaxial cell to the bottom plate.
g) Place the dual VDT's into their holders, place the extensions in place using potters clay to assure no movement during the test, and

adjust the LVDT's so that the linear range is maximized. (This is usually achieved by measurement so that each LVDT's core is equidistant from its shaft)

h) Attach back pressure line to the triaxial cell. Specimen is now ready for testing.

i) Microcomputer software package is now activated and cyclic testing is completed through response to computer prompts.

5.3.4. Resilient Modulus Test Results

The average values of the subgrade resilient moduli from lab testing are shown in Table 5-5. The laboratory test specimens were subjected to a range of confining stress as well as deviator stress in order to assess sensitivity to both types of stress. The values shown in Table 5-5 represent the average of all the test values for the various levels of stress.

A more detailed listing of the test results is given in Appendix D. For each combination of confining stress and deviator stress a best estimate value of modulus was determined. The range shown in Appendix D for each of these moduli corresponds to the range of reasonable interpretations that could be applied in computing the moduli from the hysteresis loops obtained.

The data in Table 5-5 show that the lab moduli vary from about 6.4 to 16 ksi. These values are reasonable for moduli of the materials encountered in this study. The comparisons of lab and NDT back-calculated moduli are discussed in Chapter 6. The stress level sensitivity indicated by these lab tests is discussed in Chapter 6 as well. The Atterberg limits of subgrade materials at various sites are shown in Table 5-6. Table 5-7 shows other subgrade material properties as well as R-values reported by ADOT using samples combined from different depths.

TABLE 5-5. SUMMARY OF AVERAGE RESILIENT MODULI OF SOILS SAMPLES

Site/ Station	Sample Depth (in.)	Dry Density (pct)	Water Content (%)	Confining Stress (kPa)	Deviator Stress (kPa)	Resilient Modulus (ksi)
1/1	25-32	122.1	5.28	14-31	18-93	10.43
2/1	19-25	118.6	7.09	12-30	18-69	13.30
2/7	38-45	111.6	7.83	20-27	18-38	15.51
3/7	27-34	112.3	12.4	14-31	18-86	6.44
4/1	25-32	111.8	10.4	17-41	20-86	9.59
5/4	20-27	119.9	12.4	20-33	19-62	12.19
6	Stiff Layer					
7/4	27-34	120.0	9.23	15-77	19-77	11.36
8/1	31-38	112.88	11.1	21-29	19-47	7.99
9/1	50-57	104.2	22.8	26-31	19-71	16.14
10/4	44-51	97.0	25.9	25-33	21-49	12.48
11/1	12-19	122.8	2.21	16-48	19-80	13.33
12/1	32-39	120.3	8.56	15-25	18-58	7.41
13/4	13-20	110.4	8.81	12-25	20-65	14.35
14/4	12-19	101.7	15.4	9-22	19-58	10.42
15	Bad Samples					
16/1	17-24	117.7	7.9	12-25	20-61	9.59
17/1	20-26	104.9	17.8	12-25	20-57	4.82
18	Bad Samples					
19/1	23-30	104.2	22.7	15-27	20-55	12.01
19/4	31-38	96.3	28.9	15-27	19-53	15.64
20	Bad Samples					

TABLE 5-6. ATTERBERG LIMITS OF SUBGRADE MATERIALS

Site/Station	Depth(in.)	LL	PI	Classification
1/1	25-32	18	5	SC-SM
1/4	25-32	--	NP	SM
2/1	19-25	31	5	SM
3/7	27-34	18	NP	SM
4/1	24.5-31.5	--	NP	SM
5/4	20-27	22	NP	SM
5/4	27-34	17	NP	SM
7/4	27-34	15	NP	SM
8/1	31-38	--	NP	SM
9/1	50-57	49	27	CL-CH
10/4	44-51	62	38	CH
11/1	11.5-18.5	23	5	SC-SM
11/1	18.5-25.5	--	NP	SM
12/1	32-39	20	5	SC-SM
13/4	13.5-20	28	13	SC
14/4	11.5-18.5	65	31	SC-CH
15/4	14-24	--	MP	SM
16/1	12.5-24	--	NP	SM
17/1	12-20	--	NP	SM
18/1	30-36	--	NP	SM
18/4	30-36	--	NP	GM
19/1	16-30	--	NP	SM
20/1	36-42	--	NP	GP

Note: An attempt was made to measure LL, even when the soil was too non-plastic to measure PL. For several soils, neither LL nor PL could be measured because of non-plasticity.

TABLE 5-7. SUBGRADE PROPERTIES AS REPORTED BY ADOT

Site	Depth (ft)	LL	PI	Sand Equipment	% Passing 200	Laboratory R-Value	AASHTO Classification
1	Combined	26	9	17	26	52	A-2-4(0)
2	5-6	22	1	-	45	-	A-4 (2)
2	Combined	24	3	21	21	63	A-1-b (0)
2	"	29	8	16	21	58	A-2-4 (0)
3	"	21	3	3	49	34	A-4 (3)
4	1-3	21	2	-	23	-	A-2-4 (0)
4	3-10	34	19	2	68	13	A-6 (6)
5	Combined	21	2	14	19	74	A-2-4 (0)
7	1-5	19	2	14	24	75	A-2-4 (0)
7	5-10	32	16	3	50	23	A-6 (5)
8	-	31	4	3	60	34	A-4 (5)
9	-	44	26	9	65	18	A-7-b (7)
11	3-9	28	4	15	40	53	A-4 (1)
12	Combined	19	4	20	24	57	A-1-b (11)
14	"	53	31	10	49	15	A-7-b (11)
15/1	"	21	3	20	25	67	A-1-b (0)
16	"	28	6	20	31	60	A-2-4 (0)
18	"	22	3	15	21	72	A-1-b (0)
19	-	30	1	-	44	-	A-4 (2)
20	-	23	1	16	14	82	A-1-a (0)